



FACULTY OF SCIENCE
Charles University

Habilitation thesis

Peter Košovan

Acid-base equilibria at the nanoscale

Faculty of science

Prague 2021

To my children, Lukáš, Anna and Eliška, and to my wife, Jitka. Finishing this work would be impossible without their support and patience.

Contents

Preface	3
1 Introduction	5
2 Methods for molecular simulations of acid-base equilibria	7
2.1 Overview of approaches	7
2.2 Constant-pH ensemble (cpH)	7
2.3 Reaction-ensemble Monte Carlo (RxMC)	9
2.4 Grand-reaction ensemble (G-RxMC)	9
2.4.1 The input Parameters	10
2.4.2 Acid/Base Ionisation Reaction	11
2.4.3 Connecting the System to the Reservoir	11
2.5 When to choose which method	12
3 Acid-base equilibria in solutions	15
3.1 Homogeneous systems	15
3.1.1 Ionization of an ideal weak acid and base	15
3.1.2 Ionization of a non-ideal weak acid	16
3.2 Nano-heterogeneous systems	17
3.2.1 Effect of electrostatics on the ionisation	17
3.2.2 Ionisation of a weak acid attached to a polyelectrolyte	19
3.2.3 Ionisation of weak polyelectrolytes	20
3.2.4 Ionisation of weak polyampholytes	21
4 Acid-base equilibria in two-phase systems	27
4.1 The Donnan equilibrium	28
4.1.1 Effect of electrostatics on the Donnan partitioning	30
4.1.2 Polyelectrolyte hydrogels in salt solution	32
4.2 Acid-base equilibrium coupled to a reservoir	33
4.2.1 Weak polyacid coupled to a reservoir	34
4.2.2 pH-controlled phase separation	37
5 Conclusions and outlook	41
Included publications	43
References to other works	45

Preface

This habilitation provides a selection of research results on acid-base equilibria in polyelectrolyte systems, obtained by the author and his collaborators between the years 2010 and 2021. We start by introducing the simulation methods, including the grand-reaction method that is an important result of our own research. To illustrate the evolution of our understanding of the topic, we start the presentation of results by the conceptually simplest case of an ideal weak acid in solution. Building on the concepts introduced for the ideal case, we add complexity by considering highly non-ideal solutions of weak polyacids and weak polyampholytes. Finally, we discuss the most complex case of acid-base equilibria in two-phase systems containing polyelectrolytes, exchanging small ions with the supernatant solution (reservoir). In addition to the features of acid-base equilibria in polyelectrolyte solutions, the two-phase systems are affected by the Donnan partitioning of small ions, in particular the H^+ ions.

The results presented here could have been obtained with a significant contribution from other collaborators, whose role in this work should be acknowledged. In the first place, there are master and PhD students, who have done the research work as a part of their master or PhD research projects: Roman Staňo, Raju Lunkad, Jonas Landsgesell, Tobias Richter, Anastasiia Murmiliuk, Anastasiia Fanova. Postdocs and senior colleagues whose contributions are included: Oleg Rud, Lucie Nová, Pascal Hebbeker, Filip Uhlík, Miroslav Štěpánek, Karel Procházka and Zuzana Limpouchová. Other colleagues from the Sot Matter group deserve an acknowledgment too, especially Pavel Matějčík, Mariusz Uchman and their students. The results of their work are not directly included in this text, however, they are included indirectly through numerous discussions, which influenced my view of the research topic. The PhD students Finally, I would like to acknowledge the contribution of my international collaborators and mentors at various stages of my research career: Christian Holm, Oleg Borisov and Frans Leermakers.

1. Introduction

Acid-base equilibria are ubiquitous in Chemistry, both in everyday routine work and in research. They are taught in secondary-school courses of Chemistry and then again later, in undergraduate courses of General Chemistry, Analytical Chemistry and Physical Chemistry. The basic concepts of acid, base, pH and the degree of ionisation are well established and familiar to every chemist. Nevertheless, a lot of confusion appears when these concepts are applied to complex systems on the nanoscale, such as solutions of polyelectrolytes, ampholytes, self-organized polymer nanostructures, polymers at interfaces or two-phase systems containing macromolecules.

When treating acid-base equilibria on the undergraduate level, ideal-gas approximation is often used as the starting point, leading to the Henderson-Hasselbalch equation as the main results. The activity coefficients are often introduced as small correction factors on the order of unity, which need to be considered only at high ionic strength. In the case of polyacids, polybases or polyampholytes, containing many ionisable groups within one molecule, activity coefficients can attain any values between 10^{-3} and 10^{+3} , dramatically affecting the acid-base properties of such systems. Similarly, electroneutrality is often introduced as a fundamental constraint in simplified treatments. However, it is not strictly obeyed at the nanoscale, resulting in local concentration gradients of many species, including H^+ ions, often incorrectly termed the "local pH".[2, 3] In this work, we present a compilation of simulations and experimental studies of acid-base equilibria in various macromolecular systems, in which the commonly employed simplifications are not applicable. Thereby, we provide a theoretical basis for interpreting experimental observations of acid-base equilibria in such systems.

The acid-base properties of molecules with many titratable groups are very different from low-molecular weak acids or bases with a small number of titratable groups. For acids with few titratable groups (e.g., oxalic acid or phosphoric acid), different pK_A values can be assigned to each ionisation state because the titration curve contains several distinct inflection points. However, a macromolecule with n identical ionisable groups has 2^n distinct ionisation states. This number of distinct states becomes too large, greater than the number of points on an experimentally determined titration curve, already at a rather small $n \gtrsim 10$, . Therefore, titration curves of synthetic polymers, such as poly(acrylic) acid, vary smoothly across a broad range of pH, thus making it practically impossible to assign a specific pK_A to each state. Consequently, a different approach is needed to describe their acid-base properties.

The acid-base properties of charged macromolecules are predominantly affected by electrostatic interactions between ionised groups.[9, 10, 11, 12, 13, 14] The general notion is that repulsion between like-charged groups suppresses ionisation, while attraction between oppositely charged groups enhances ionisation. The net result depends on the pK_A of each individual group and on the distribution of ionisable groups in space. This electrostatic effect on the ionisation should be distinguished from the effect of replacing local substituents upon incorporation of the ionisable monomer in the polymer. The latter affect the pK_A by changing the electron density in the chemical bonds close to the titratable group. Often, these changes are described in terms of the effective acidity constant, pK_{eff} , that is generally different from the *bare* pK_A of the parent monomer. The main drawback of using pK_{eff} is that it is not a constant but an effective parameter that depends on all other parameters. For example, pK_{eff} of poly(acrylic acid), which is often viewed as a typical weak polyelectrolyte, varies between the bare $pK_A = 4.25$, and $pK_{\text{eff}} \approx 8.0$, depending on the pH, salt concentration, or molar mass of the polymer.[13, 15] Also in protein research, deviations from

the ideal ionisation response of individual titratable groups are commonly expressed in terms of their effective pK_A . Nevertheless, it has been generally recognized that such a description, using a single number as an effective parameter, is not sufficient to describe the complex acid-base equilibria in proteins. On the semi-empirical level, this problem has been solved by employing the Hill equation, and introducing the Hill coefficient as an adjustable parameter that improves the agreement between the theory and experiment. Furthermore, it has been recognized that the bare pK_A values of amino acids in proteins are different from those of free amino acids in solution.[16, 17] Thus, in spite of the obvious drawbacks, the effective acidity constants are widely used in contemporary scientific literature.

The aim of this work is to provide an alternative view of the same problem. Instead of predicting effective constants, that are actually not constant at all, we use computer simulations to predict how the total charge on polyelectrolytes, ampholytes or short peptides depends on the pH. By inspecting the ionisation degrees of individual acid or base groups, predicted from the simulations, we can obtain a mechanistic understanding of the factors affecting their ionisation response as a function of pH.

Changes in pH can be used to control enzyme activity or protein aggregation[18, 19], to trigger the release of anti-cancer drugs[20] or to control protein sequestration in polyelectrolyte brushes, gels and complexes[21, 22, 23], as shown by the rapid development of pH-responsive materials, and their applications.[24] The macromolecular systems, used in these applications, are often too complicated to be fully understood. Consequently, these systems are often optimized based on a trial-and-error strategy, because their fundamental understanding is very limited. By using simple model systems, it is possible to bridge the gap between the excessively complex systems used in real applications, and oversimplified models used in many theories. Computer simulations, presented in this work, provide the the missing piece in the puzzle – the fundamental understanding of the relevant mechanisms affecting acid-base equilibria in complex macromolecular systems.

2. Methods for molecular simulations of acid-base equilibria

Description of methods in this chapter largely follows the original text of Ref.[4] (Sections 2.2, 2.2 and 2.3) and Ref.[5] (Section 2.4). The description of methods is included mainly for completeness, in order to provide a consistent methodological context for the reader. Nevertheless, the Grand-reaction method, introduced in Section 2.4, is an original result of our work, and an important milestone in method development that enabled simulations of a broad class of reactive systems. A reader interested mainly in the results may skip this section.

2.1 Overview of approaches

We focus on two main simulation approaches (thermodynamic ensembles) that have been used for simulating weak polyelectrolytes in our work: The Reaction Ensemble Monte-Carlo method (RxMC) and the constant-pH method (cpH). The former has been further extended by explicit coupling to a reservoir, termed the Grand-Reaction method (G-RxMC). These methods are available in the simulation package ESPResSo [25] that has been used also for most simulations presented in this work.

Several other methods have been formulated for simulating ionisation reactions[26, 27, 28, 29, 30]. These include for example the lambda dynamics[31], the reactive force field[32], and various variations of RxMC or cpH methods with enhanced sampling schemes and modified acceptance probabilities[33, 34]. However, we will not discuss them in detail here because they are not directly related to our results. For detailed information, we refer the reader to the original articles or specialized reviews[35, 36, 34, 37, 38, 39].

Both RxMC and cpH methods combine sampling of the conformational space at a fixed chemical composition (configuration moves) with sampling the reaction coordinate at a fixed system conformation (reaction moves). By construction, both these methods are Monte Carlo methods, implementing stochastic processes to represent the reactions. They have been used in combination with sampling of the configuration space by means of Langevin dynamics. Because the algorithms for sampling polymer conformations are widely established techniques, we will not discuss them here. However, the reaction moves are rather specific, and they constitute the essential feature of simulations of acid-base equilibria presented here. These are Monte-Carlo moves in which a chemical change is proposed, defined by the chemical reaction under study. The proposed change is accepted with a specific acceptance probability, in analogy with the usual Metropolis scheme described in simulation textbooks[40]. In the following paragraphs, we describe how the reactions are proposed and accepted.

2.2 Constant-pH ensemble (cpH)

Introduced by Reed and Reed[41], the constant-pH ensemble assumes a system in a solution at a fixed chemical potential of H^+ ions, which is defined by the pH value. The constant-pH method assumes a dissociation reaction of a weak acid or a weak base



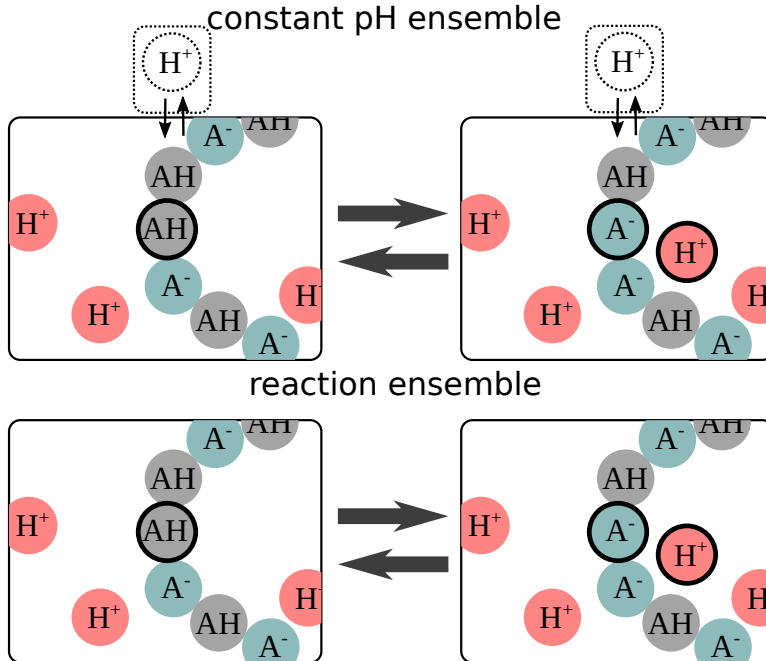


Figure 2.1: Schematic representation of the constant-pH ensemble and the reaction ensemble setup. Reproduced from Ref.[4] with permission from The Royal Society of Chemistry.

In further text, we will discuss only the acid dissociation because the base reaction is analogous.

In a constant-pH simulation, the dissociation reaction is proposed with a probability proportional to the amount of associated species HA, while the association reaction is proposed proportional to the amount of dissociated species, A^- . In the forward direction of the reaction in (2.1), the identity of a randomly selected HA particle is changed to A^- , and an additional H^+ ion is inserted at a random position in the system. In the reverse direction, a randomly selected A^- is changed to HA and one H^+ ion is deleted from the system. The acceptance probability follows as [41],

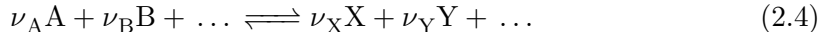
$$P_{\text{on}}^{\text{cpH}} = \min \left[1, \exp \left(-\beta \Delta U_{\text{on}} + \xi (\text{pH} - \text{p}K_A) \ln(10) \right) \right], \quad (2.3)$$

where $\beta = 1/k_B T$, $\Delta U_{\text{on}} = U_n - U_o$ is the interaction energy change between the old state (o) and the new state (n), and $\xi = \pm 1$ is the extent of reaction that corresponds to one reaction step in the forward or reverse direction, respectively.

Methods based on the same key idea as the cpH ensemble have been introduced by various authors under different names and with slight variations of the reaction move and acceptance probabilities. For example, a formulation with a symmetric proposal probability can be found in Ref.[42]. Panagiotopoulos used an analogous method, derived from the grandcanonical ensemble[43]. Uyaver and Seidel[44, 45, 46], as well as Stoll and coworkers[47, 48, 49, 50] referred to the same method as the grandcanonical or semi-grandcanonical ensemble. The constant-pH method and its close relatives are particularly popular in biomolecular simulations for calculating protonation states of amino acid residues in proteins, and numerous improvements have been introduced in this context[38].

2.3 Reaction-ensemble Monte Carlo (RxMC)

The reaction ensemble Monte-Carlo (RxMC) method has been independently introduced by two groups, by considering all-atom simulations of gas-phase reactions[51, 52]. Unlike the cpH method, the RxMC method can be used to model an arbitrary chemical reaction, schematically written as



Where $\{A, B, X, Y\}$ denote arbitrary reactants or products, and ν denotes their stoichiometric coefficients. In the current context, we will apply the RxMC formalism to the special case of acid-base reactions in solutions.

In the RxMC method, the chemical reaction is performed by insertion, deletion, or modification of chemical identity of the relevant species. Specifically, in the forward direction of the reaction (2.1), the identity of a randomly selected HA is changed to A^- , and an additional H^+ ion is inserted at a random position in the system. In the reverse direction, a randomly selected A^- is changed to HA and one H^+ ion is deleted from the system. The forward and reverse direction of the reaction are both proposed with the same probability. The original articles[51, 52] derived the following acceptance probability for such a reaction move:

$$P_{\text{on}}^{\text{gas}} = \min \left\{ 1, (V^{\bar{\nu}} \Gamma)^{\xi} \prod_i \left[\frac{(N_i^0)!}{(N_i^0 + \nu_i \xi)!} \right] \exp(-\beta \Delta U_{\text{on}}) \right\}, \quad (2.5)$$

where N_i^0 is the number of species i before the attempted transition. The equilibrium constant, Γ , is related to the concentration-based equilibrium constant K_c (3.11),

$$\Gamma = \prod_i \left(\frac{N_i}{V} \right)^{\nu_i} = K_c N_A^{\bar{\nu}}, \quad (2.6)$$

where N_i is the average number of species i in the simulation box and N_A is the Avogadro constant. The acceptance probability can be rewritten in terms of K_c :

$$P_{\text{on}}^{\xi} = \min \left\{ 1, \left(K_c (V N_A)^{\bar{\nu}} \right)^{\xi} \prod_i \left[\frac{(N_i^0)!}{(N_i^0 + \nu_i \xi)!} \right] \exp(-\beta \Delta U_{\text{on}}) \right\}. \quad (2.7)$$

or in terms of the dimensionless reaction constant K

$$P_{\text{on}}^{\text{RxMC}} = \min \left\{ 1, \left(K (c^{\ominus} V N_A)^{\bar{\nu}} \right)^{\xi} \prod_i \left[\frac{(N_i^0)!}{(N_i^0 + \nu_i \xi)!} \right] \exp(-\beta \Delta U_{\text{on}}) \right\} \quad (2.8)$$

where

$$k_B T \ln K = \sum_i \nu_i \mu_i^{\ominus} \quad \text{and} \quad K = K_c (c^{\ominus})^{\bar{\nu}} \quad (2.9)$$

It follows from the above that the inputs of an RxMC simulation comprise the equilibrium reaction constant and the initial composition of the reacting mixture. Outputs of the RxMC simulation comprise equilibrium concentrations of individual reacting species.

2.4 Grand-reaction ensemble (G-RxMC)

Both above-mentioned methods, cpH and RxMC, deal with chemical reactions in closed systems, whereas many chemical reactions in macromolecular systems occur in partial-open systems. In such systems, some components, typically inorganic ions or small

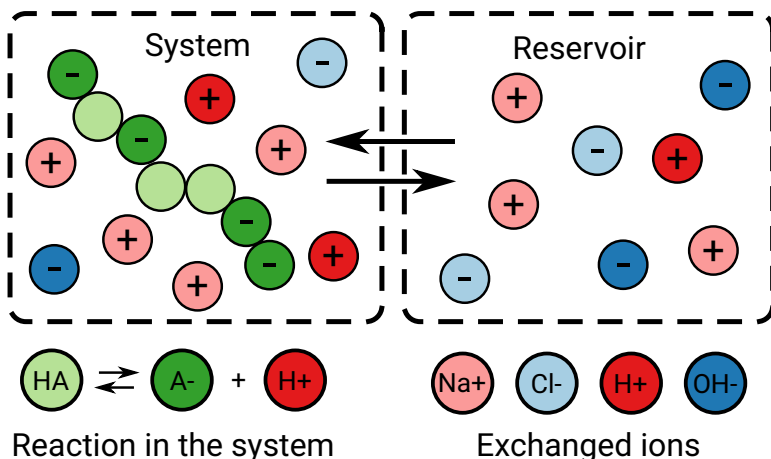


Figure 2.2: Schematic representation of the grand-reaction ensemble setup Reprinted with permission from Ref.[5]. Copyright (2020) American Chemical Society.

molecules, can be exchanged with the surrounding solution (reservoir), while other components, typically macromolecules, are present only in the system but cannot be exchanged with the reservoir, as illustrated in Fig.2.2. To enable coarse-grained simulations of such systems, we introduced the Grand-reaction ensemble (G-RxMC) in 2020[5]. The G-RxMC method provides a general approach to simulating multi-component reaction equilibria in a system coupled to a reservoir, with which the simulated system can exchange some but not all of its constituents. In this text, we specifically focus on its use for coarse-grained models representing an aqueous solution of ions in an implicit solvent that is treated as a continuum, characterized by the relative permittivity, ϵ_r .

2.4.1 The input Parameters

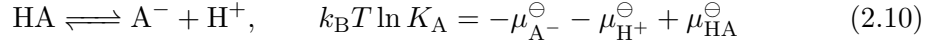
The simulated system is defined by specifying its temperature T , volume V , concentrations c of components that cannot be exchanged with the reservoir, and chemical potentials μ of those components that exchange be exchanged with the reservoir. Alternatively, we can specify concentrations of the reservoir constituents and determine their chemical potentials. Furthermore, we specify the chemical reactions that occur in the system by their stoichiometry and by their equilibrium reaction constants K . In the general case, the reservoir may consist of an arbitrary number of constituents, and the chemical reactions can involve arbitrary constituents of the system.

We apply this general framework to a solution of weak polyelectrolytes composed of N identical segments, in equilibrium with a salt solution at a given pH and composition. Chemical reactions in our system comprise the acid-base ionisation of the weak polyelectrolyte, characterized by the acidity constant K_A . In this example, the polymer chains represent the components that are not exchanged with the reservoir, whereas the H^+ , Na^+ , Cl^- , and OH^- ions represent the constituents that are exchanged with the reservoir. In an aqueous reservoir containing n ionic constituents, only $(n-2)$ chemical potentials can be specified independently. The two remaining chemical potentials follow from the electroneutrality constraint, and from the ionic product of water. In the simulation model, all involved constituents are described by some short-range repulsive interaction potential and by the valency which determines their electrostatic interactions. The exact form of short-range potentials may differ, depending on the specific model, but it is unimportant in the current context. The simulation combines sampling of the simulated system in several orthogonal directions: (i) sampling the system configurations while maintaining a fixed composition; (ii) sampling the composition

fluctuations due to chemical reactions and (iii) sampling the composition fluctuations due to exchange of particles with the reservoir.

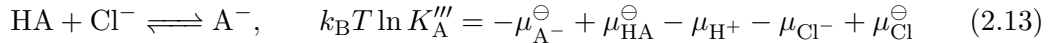
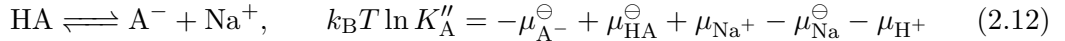
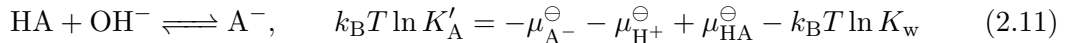
2.4.2 Acid/Base Ionisation Reaction

Chemical reactions in the system are simulated using the RxMC method. When considering a coarse-grained model in implicit solvent, it is important to note that the acid-base reactions involve a reaction with water, while water molecules are not treated explicitly in the implicit-solvent representation. This requires special caution when setting-up the reactions. The acidity constant, K_A , is the equilibrium constant of the ionisation reaction (2.1)



Where μ_i denotes the chemical potential and μ_i^\ominus denotes the reference chemical potential of species i . By convention, the chemical potential of water is assumed to be constant and included in the definition of K_A . Although the water molecules are not represented by explicit particles, they participate in the acid-base ionisation. Therefore, the H^+ and OH^- ions produced by the ionisation reactions must be represented explicitly.

The acid ionisation reaction, (2.1), can be conveniently simulated using the reaction ensemble at $\text{pH} \lesssim 4$. At $\text{pH} \gtrsim 4$, the concentration of H^+ is so low that with a typical simulation box size, $L \approx 20$ nm, one obtains less than one H^+ ion per simulation box, and the reaction ensemble simulation becomes very inefficient. To avoid this bottleneck, we re-formulated the ionisation reaction using other ions, and modified the equilibrium constants accordingly.



The reactions (2.11)–2.13 can be formally derived as the net result of combining (2.10), representing the ionisation reaction, with (2.14–2.17), representing the ion-exchange with the reservoir, as defined in the next section. Note that only K_A and K'_A are true equilibrium constants because they depend only on the reference chemical potentials. On the contrary, constants K''_A and K'''_A depend on the reservoir composition *via* ($\mu_{\text{Na}^+} - \mu_{\text{H}^+}$) and ($\mu_{\text{H}^+} - \mu_{\text{Cl}^-}$), respectively.

2.4.3 Connecting the System to the Reservoir

To couple the simulated system to the reservoir, we implemented the Grand-canonical exchange of particles with a reservoir, as described in various textbooks.[40, 53] It is convenient to write these particle insertions and deletions as chemical reactions in which particles are created (inserted) in the simulation box or removed (deleted) from the simulation box. To retain the electroneutrality of the simulation box, we always insert or delete an electroneutral ion pair. Specifically, to simulate particle exchange with a reservoir consisting of Na^+ , Cl^- , H^+ and OH^- ions, we define the following reactions (ion pair insertions):

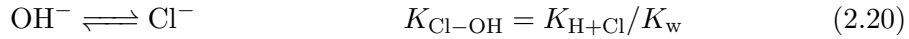
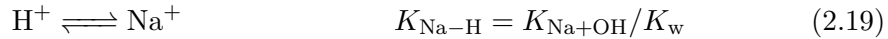


where K_w is the ionic product of water, and we define the remaining equilibrium constants in Equations (2.14 – 2.17) as $k_B T \ln K_{i+j} = (\mu_i - \mu_i^\ominus) + (\mu_j - \mu_j^\ominus)$. The above equations are not independent because adding (2.14 + 2.17) is equivalent to adding (2.16 + 2.15), thereby resulting in the following stoichiometry constraint, equivalent to imposing electroneutrality of the reservoir:

$$K_{\text{Na+Cl}} K_w = K_{\text{H+Cl}} K_{\text{Na+OH}} \quad (2.18)$$

Since K_w is fixed, only two of the three remaining constants can be chosen independently to uniquely determine the system composition. In our case, we specify the remaining two degrees of freedom by setting the pH and the concentration of added salt in the reservoir.

As an alternative to inserting or deleting ion pairs, particle identities can be exchanged, which is formulated as reactions formally obtained by subtracting (2.16 – 2.17) and (2.15 – 2.17)



where $k_B T \ln K_{i-j} = (\mu_i - \mu_i^\ominus) - (\mu_j - \mu_j^\ominus)$.

Linking the reservoir chemical potentials, its composition and pH

In experiments, it is often convenient to characterize the reservoir by its composition, for example, by specifying the amount of NaCl that has been dissolved in water and the amount of NaOH or HCl that has been added to adjust the pH. Conversely, our simulation algorithm requires chemical potentials of the reservoir constituents as inputs. The relationship between the composition and the chemical potentials in a reservoir consisting of interacting particles is unique but complex. Therefore, we can either specify the chemical potentials and determine the reservoir composition from an auxiliary simulation, or we can specify the compositions, and determine the corresponding chemical potentials from a simulation.

If we characterize the reservoir by choosing the chemical potentials, we can choose two of the chemical potentials $\{\mu_{\text{Na}^+}, \mu_{\text{Cl}^-}, (\mu_{\text{H}^+} \text{ or } \mu_{\text{OH}^-})\}$, or equivalently two of the reaction constants $\{K_{\text{Na+Cl}}, K_{\text{H+Cl}}, K_{\text{Na+OH}}\}$. The salt concentration in the reservoir then corresponds to the number of NaCl ion pairs, that is, $c_{\text{salt}}^{\text{res}} = \min(c_{\text{Na}^+}^{\text{res}}, c_{\text{Cl}^-}^{\text{res}})$. The reservoir pH follows directly from μ_{H^+} . Depending on the pH, we can calculate the concentration of additional NaOH or HCl, required to reach this pH value.

If the reservoir is defined by its composition, then μ_i^{id} is known for all species, and μ_i^{ex} should be determined in an auxiliary simulation of the reservoir alone by directly calculating μ^{ex} using the Widom particle insertion[40]. In particular, the reservoir pH is not known a priori and must be determined by calculating μ_{H^+} at the given concentration of H^+ ions and reservoir composition. Only then, the difference $\mu_i - \mu_i^\ominus = \mu_i^{\text{id}} + \mu_i^{\text{ex}}$ can be computed, which is the required input parameter of the acceptance probability. To ensure that the constraint $k_B T \ln K_w = \mu_{\text{H}^+} + \mu_{\text{OH}^-}$ is satisfied, the reservoir concentration of H^+ or OH^- should be adjusted iteratively, based on the calculated μ^{ex} . This is especially important if the reservoir ionic strength, I^{res} , is dominated by the H^+ or OH^- ions, that is, if $\text{pH} \lesssim -\log_{10} c_{\text{salt}}^{\text{res}}/c^\ominus$, or $\text{pOH} \lesssim -\log_{10} c_{\text{salt}}^{\text{res}}/c^\ominus$.

2.5 When to choose which method

In the constant-pH ensemble, one specifies the pH and concentration of the ionisable species as inputs, and obtains the degree of ionisation, as well as ensemble averages

of observables at a given system composition and at a given pH, as an output. Experimentally, this cpH ensemble could be realized as a solution of a weak acid in an excess of a buffer that keeps the pH at a constant value, effectively having an infinite buffer capacity. However, the H^+ ions and OH^- ions of this buffer are not represented explicitly. In fact, their concentrations are treated as free parameters that are not coupled to the pH value specified as the input. This is a reasonable approximation in the intermediate pH range, if the H^+ and OH^- ions are minority species, and their contribution to properties of the solution can be neglected. However, this approximation breaks down at a high or low pH value, if simultaneously the ionic strength is low enough, such that the H^+ or OH^- ions become the majority species. Thus, the "safe range" of the constant-pH method can be defined as $\text{pSalt} < \min(\text{pH}, \text{pOH})$ where $\text{pSalt} = -\log_{10} c_{\text{salt}}^{\text{res}}$. Additionally, the constant-pH approximation breaks down if the concentration of ionisable groups in the simulated system is comparable to the ionic strength of the solution. In such case, the (hypothetical) buffer cannot be assumed to have an infinite buffering capacity, and the effect of the ionisation state on the solution pH should be considered explicitly.

The standard reaction ensemble setup corresponds to a chemical reaction performed in a closed system, where the total number of reacting species (atoms) is conserved, but they can be rearranged into species of different chemical identities (molecules). Experimentally this ensemble could be realized by mixing two solutions of known initial composition, and measuring the resultant pH and equilibrium composition after the reaction. The pH is not directly set as input of the RxMC simulation. It is obtained as its output, same as in the experiment. However, the desired pH can be chosen indirectly by using a suitable initial composition of the system. The RxMC method requires a sufficient number of H^+ or OH^- ions in the simulation box, which is easily achieved at high or low pH values. On the contrary, the RxMC method is impractical in the range $3 \lesssim \text{pH} \lesssim 11$ because it would require very big simulation boxes in order to obtain a sufficient number of H^+ or OH^- ions.

It follows from the above considerations that both cpH and RxMC methods are suitable for simulating a one-phase system, such as a polyelectrolyte solution in a buffer. In principle, the cpH and RxMC methods should yield very similar results under the same conditions. Therefore, the suitability of cpH or RxMC method for a particular problem is determined mainly by practical considerations described above. In contrast with the cpH and RxMC methods, in the G-RxMC method one specifies the properties of the reservoir (pH, salt concentration), and obtains pH and ionisation degree inside the system as a simulation result. Therefore, the G-RxMC method is the only one that is suitable for situations, where partitioning of ions between the system and the reservoir plays an important role. Examples of such systems include not only polyelectrolyte or protein solutions separated from the reservoir by a semipermeable membrane, but also membrane-less two-phase systems, such as polyelectrolyte hydrogels, electrostatically crosslinked reversible gels, or complex coacervates in contact with a supernatant solution of small ions.

3. Acid-base equilibria in solutions

We start the discussion of results by introducing the terminology and presenting some established equations for the ionisation behaviour of weak acids and bases in homogeneous systems, where all ionisable groups are equivalent. These results will serve as a starting point for the subsequent discussion of nano-heterogeneous macromolecular systems in which the ionisation state of each acid or base group depends not only on macroscopic parameters (pH, ionic strength) but also on its position within a polymer chain.

3.1 Homogeneous systems

3.1.1 Ionization of an ideal weak acid and base

In analogy with an ideal gas, we will use the terms ideal acid and ideal base to describe the situations in which we neglect intermolecular interactions. The ionisation of an acid HA and base B can be described by the following reactions and their equilibrium constants:



where A^- and BH^+ represent their ionised forms. Note that (3.1) is identical to (2.1), and (3.2) is identical to (2.2). We re-state these reactions in this chapter just to ensure better readability. In the ideal case, the (dimensionless) equilibrium constants can be expressed in terms of concentrations

$$K_{\text{A}}^{\text{acid ideal}} \equiv \frac{c_{\text{A}^-} c_{\text{H}^+}}{c_{\text{HA}} c^{\ominus}} \quad K_{\text{A}}^{\text{base ideal}} \equiv \frac{c_{\text{B}} c_{\text{H}^+}}{c_{\text{BH}^+} c^{\ominus}}. \quad (3.3)$$

We define the degree of ionization α as the fraction of ionized groups of a given type. It is convenient to introduce the degree of ionization,

$$\alpha_{\text{acid}} \equiv \frac{c_{\text{A}^-}}{c_{\text{A}^-} + c_{\text{HA}}} \quad \alpha_{\text{base}} \equiv \frac{c_{\text{BH}^+}}{c_{\text{BH}^+} + c_{\text{B}}}. \quad (3.4)$$

In the ideal case (in the absence of interactions), the degree of ionisation, α , of each ionisable group depends only on the difference $\text{pH} - \text{p}K_{\text{A}}$ via the Henderson-Hasselbalch equation:

$$\text{pH} - \text{p}K_{\text{A}}^{\text{acid}} = \log_{10} \frac{\alpha}{1 - \alpha}, \quad \text{pH} - \text{p}K_{\text{A}}^{\text{base}} = \log_{10} \frac{1 - \alpha}{\alpha} \quad (3.5)$$

where we introduced the logarithms of equilibrium constants, $\text{p}K_{\text{A}}^{\text{acid}} = -\log_{10} K_{\text{A}}^{\text{acid}}$ and $\text{p}K_{\text{A}}^{\text{base}} = -\log_{10} K_{\text{A}}^{\text{base}}$. For completeness, we add that if a molecule consists of multiple ionizable groups with different $\text{p}K_{\text{A}}$ values, its total charge z at a given pH is given by

$$z(\text{pH}) = \sum_i n_i \alpha_i(\text{pH}) z_i \quad (3.6)$$

where n_i is the number of groups of type i in the molecule, α_i is their average degree of ionisation, and $z_i = \pm 1$ is their charge in the ionised state. In a polyelectrolyte,

the degree of ionization of various chemically identical monomer units depends also on their position in the chain. Unless specified otherwise, we assume that α refers to the degree of ionization averaged over all chemically equivalent ionisable groups, irrespective of their position in the macromolecular chain. In further text, we will describe in detail only the ionisation of acids, assuming that the behaviour of bases follows from a straightforward analogy.

3.1.2 Ionization of a non-ideal weak acid

In contrast with the ideal case, when describing a non-ideal acid or base, we take intermolecular interactions into account, that affect the ionisation state. General Chemistry textbooks teach us that the ionization of monoprotic acids approaches the ideal behaviour at high dilution. Deviations from this ideal behaviour occur at rather high ionic strengths, $I \gtrsim 10^{-2}$ M, due to ionic screening, as described by the Debye-Hückel theory. In other words, the ionisation of low-molecular monoprotic acids deviates from the ideal behaviour predominantly due to their interactions with salt ions in the solution, forming the ionic atmosphere. In contrast with that, the ionisation of multiprotic acids, bases or ampholytes with multiple ionisable sites, deviates from the ideal behaviour predominantly due to interactions between the ionised groups within the same molecule. Often, such titration curves are described using an effective acidity constant, pK_{eff} , defined as the pH at which the ionisable groups are 50% charged, on average. However, a single value of pK_{eff} is insufficient to describe the non-uniform deformation of the dependence of ionization degree on pH[2, 54, 55].

In spite of the above, there are specific situations when one value of pK_{eff} appropriately describes the shift of the ionisation response of a weak acid, for example if it is attached to a strong polyelectrolyte or to a charged surface with a constant charge that does not depend on pH[12, 3]. To describe such non-ideal ionization we start from the general condition of chemical equilibrium for any chemical reaction,

$$0 = \sum_i \nu_i \mu_i = \sum_i \nu_i \left(\mu_i^\ominus + \mu_i^{\text{id}} + \mu_i^{\text{ex}} \right), \quad (3.7)$$

where ν_i is the stoichiometric coefficient of species i , and the summation index runs over all reacting species. From now on, we will discuss the special case of (3.1), so that the reacting species are defined as $i = \{\text{HA}, \text{A}^-, \text{H}^+\}$.

The chemical potential μ_i can be expressed as a sum of the reference chemical potential, μ_i^\ominus , the ideal gas chemical potential, μ_i^{id} , and the excess chemical potential, μ_i^{ex} , due to intermolecular interactions. Using these terms, We define the acidity constant, K_A , and μ_i^{id} as

$$\ln K_A \equiv -\frac{1}{k_B T} \sum_i \nu_i \mu_i^\ominus, \quad \frac{\mu_i^{\text{id}}}{k_B T} \equiv \ln \frac{c_i}{c^\ominus}, \quad (3.8)$$

where c_i is the molar concentration of species i , and c^\ominus is the reference concentration. The choice of the reference state is arbitrary and has no impact on the thermodynamics. However, it affects μ_i^\ominus , and thereby the numerical values of K_A . Using these terms, we can express the activity a_i , activity coefficient γ_i and excess chemical potential[56]

$$\ln a_i = \frac{\mu_i - \mu_i^\ominus}{k_B T}, \quad a_i = \gamma_i \frac{c_i}{c^\ominus}, \quad \mu_i^{\text{ex}} = k_B T \ln \gamma_i \quad (3.9)$$

in order to rewrite K_A in the form commonly encountered in textbooks,

$$K_A = \prod_i a_i^{\nu_i} = (c^\ominus)^{-\bar{\nu}} \prod_i (\gamma_i c_i)^{\nu_i} = \frac{a_{\text{H}^+} a_{\text{A}^-}}{a_{\text{HA}}}, \quad (3.10)$$

where $\bar{\nu} = \sum_i \nu_i$. In the absence of intermolecular interactions (ideal system, $\gamma_i = 1$), we can relate K_A to the concentration-based equilibrium constant of the reaction, K_c ,

$$K_c \equiv \prod_i (c_i)^{\nu_i} = \frac{c_{\text{H}^+} c_{\text{A}^-}}{c_{\text{HA}}} \stackrel{\text{ideal}}{=} K_A (c^\ominus)^{\bar{\nu}}. \quad (3.11)$$

We put the superscript “ideal” to remind the reader that K_c is a true constant only under ideal conditions. In this definition, K_c has the dimension of $c^{\bar{\nu}}$, and the reference concentration, c^\ominus , is absorbed in the value of K_c . However, in Physical Chemistry and Chemical Thermodynamics, the preferred convention is to define K_c as dimensionless, normalized by the reference concentration $(c^\ominus)^{\bar{\nu}}$.

Using the definitions of α , K_A and the IUPAC definition of pH[56],

$$\text{pH} = -\log_{10} a_{\text{H}^+} = \frac{\mu_{\text{H}^+}^\ominus - \mu_{\text{H}^+}}{k_{\text{B}}T \ln(10)}. \quad (3.12)$$

we can rewrite (3.7) in a form analogous to the Henderson-Hasselbalch equation, (3.5),

$$\text{pH} - \text{p}K_A = \log_{10} \frac{\alpha}{1 - \alpha} + \frac{1}{k_{\text{B}}T \ln(10)} \sum_{i \neq \text{H}^+} \nu_i \mu_i^{\text{ex}}. \quad (3.13)$$

Equation (3.13) provides a general description of a non-ideal dissociation reaction in a homogeneous system. The challenge in describing such a reaction consists in evaluating the excess chemical potentials. It is important to note that the excess chemical potential of H^+ is excluded from Equation 3.13 because it is already included in the pH, see (3.12). To simplify the notation, we introduce the term Δ that groups the remaining excess terms in (3.13)

$$\Delta = \frac{1}{k_{\text{B}}T \ln(10)} \sum_{i \neq \text{H}^+} \nu_i \mu_i^{\text{ex}}, \quad (3.14)$$

and define the effective pH and effective $\text{p}K_A$ as

$$\text{pH}_{\text{eff}} \equiv \text{pH} - \Delta, \quad \text{p}K_{\text{eff}} \equiv \text{p}K_A + \Delta. \quad (3.15)$$

Using the definitions in (3.15), we can cast (3.13) in the form

$$\text{pH} - \text{p}K_A^{\text{acid}} - \Delta = \text{pH} - \text{p}K_{\text{eff}} = \text{pH}_{\text{eff}} - \text{p}K_A^{\text{acid}} = \log_{10} \frac{\alpha}{1 - \alpha}, \quad (3.16)$$

and in an analogous form for the ionisation of a base

$$\text{pH} - \text{p}K_A^{\text{base}} - \Delta = \log_{10} \frac{1 - \alpha}{\alpha}. \quad (3.17)$$

Equation (3.16) demonstrates that we can equivalently describe the non-ideal ionization behaviour using the effective acidity constant, $\text{p}K_{\text{eff}}$, or using the effective pH, pH_{eff} , which has been first recognized by Hartley and Roe in the 1940s[12]. Although this result has been known since nearly 80 years, it still causes confusion, and this equivalence seems to be unclear to many contemporary researchers.

3.2 Nano-heterogeneous systems

3.2.1 Effect of electrostatics on the ionisation

Using the formalism introduced in Equations (3.15), (3.16) and (3.17), we can describe acid-base ionisation equilibria in inhomogeneous systems, where dominant contribution to interactions is of electrostatic origin. The mean-field description provides a relation

between the excess contribution, Δ , and the mean local electrostatic potential $\langle\psi(\mathbf{r})\rangle$ as[12]

$$\Delta = -\frac{\langle e\psi(\mathbf{r})\rangle}{k_{\text{B}}T \ln(10)}, \quad (3.18)$$

where e denotes the elementary charge. At the same time, the spatial distribution of ions of type i and valency z_i follows the Boltzmann distribution due to the spatially varying electrostatic potential

$$c_i(\mathbf{r}) = c_i^{\text{bulk}} \exp\left(\frac{\langle -z_i e\psi(\mathbf{r})\rangle}{k_{\text{B}}T}\right), \quad (3.19)$$

where c_i^{bulk} denotes concentration of species i in the bulk. The term *bulk* usually refers to a homogeneous part of the solution that is far away from the investigated object of interest. As such, it is well defined when discussing the distribution of ions at a charged surface, however, it becomes a bit fuzzy when discussing the distribution of ions at a polyelectrolyte chain in solution. Combining (3.19) and (3.18), we recognize that it is possible to use the local concentrations of individual species to account for their activities, and formulate the ionization equilibrium locally[12, 14, 57]

$$K_{\text{A}} = (c^{\ominus})^{-\bar{\nu}} \prod_i (\gamma_i c_i)^{\nu_i} = (c^{\ominus})^{-\bar{\nu}} \prod_i (c_i(\mathbf{r}))^{\nu_i}. \quad (3.20)$$

Equation (3.20) represents the core idea of treating ionization equilibria in mean-field methods. It can also be written as the local analogue of the Henderson-Hasselbalch equation[14, 58, 57, 59],

$$\frac{\alpha(\mathbf{r})}{1 - \alpha(\mathbf{r})} = \frac{K_{\text{A}} c^{\ominus}}{c_{\text{H}^+}(\mathbf{r})}. \quad (3.21)$$

The above discussion is valid as long as the mean-field approximation is applicable, *i.e.*, when the fluctuating value of $\psi(\mathbf{r})$ can well be approximated by its ensemble-averaged value, $\langle\psi(\mathbf{r})\rangle$. When fluctuations of $\psi(\mathbf{r})$ become relevant, the results remain qualitatively valid but the observed deviations from the ideal behaviour are lower than those predicted by (3.18)[3].

In a weak polyelectrolyte, each ionizable group is subject to a different electrostatic potential, depending on its position on the chain. In addition, this potential depends on the ionization of other neighboring groups. Therefore, the ionisation of weak polyelectrolytes is not only shifted with respect to the ideal case by a constant offset Δ , but it is also deformed. In such a case, analytical theory is usually insufficient, and it is necessary to resort to numerical models and computer simulations.

The “local pH”

Since the local concentration of H^+ ions reflects the (mean) local electrostatic potential, the term “local pH” has been coined, defined by some authors as

$$\text{”local pH”}(\mathbf{r}) \equiv -\log_{10} \frac{c_{\text{H}^+}(\mathbf{r})}{c^{\ominus}}. \quad (3.22)$$

In line with (3.21), this “local pH” provides an alternative description of non-ideal ionisation equilibria. We write this term in quotes to emphasize its controversy because it is in conflict with the IUPAC definition of pH (3.12), which implies that the pH value within a single-phase system is constant, independent of position. Therefore, it should be recognized that the “local pH” defined in (3.22) actually is not the local value of pH, as its name suggests. It is just a convenient abbreviation for the somewhat

lengthy term “negative common logarithm of the local concentration of H^+ ions”. This terminology might lead to confusion, for example, when discussing two-phase systems with different compartments separated by a membrane. In such a case, the local value of pH can indeed differ between the phases, in line with the IUPAC definition of pH. Despite this conflict in nomenclature, the term “local pH” is quite widespread in both theoretical and experimental literature, and often used with the implicit assumption that the reader knows what the authors mean. Therefore, we propose that the term “local pH” should be used with caution, and it should be always accompanied by an explicit definition.

3.2.2 Ionisation of a weak acid attached to a polyelectrolyte

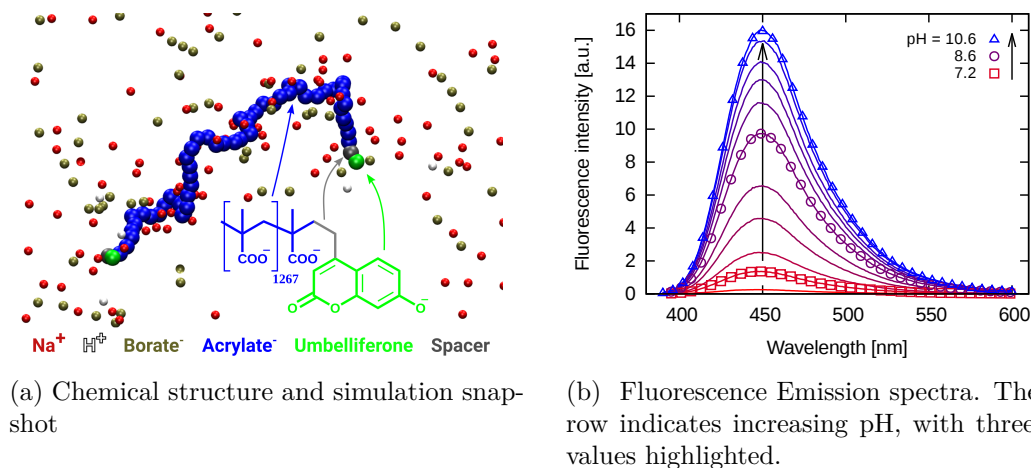


Figure 3.1: Chemical structure the Umb-PMAA polymer and simulation snapshot showing the coarse-grained representation. Fluorescence emission spectra show to response of Umb-PMAA to a variation of pH. Reprinted with permission from Ref.[3]. Copyright (2020) American Chemical Society.

The concepts introduced in Equations (3.16) and (3.19) can be used to describe the ionization of a weak acid attached to a fully charged polyelectrolyte chain, such as umbelliferone attached to poly(methacrylic acid) (PMAA), shown in Fig. 3.1a. Umbelliferone is not only a weak acid with $pK_A = 7.85$ but also a fluorescent pH indicator, therefore, its ionisation at various pH can be followed by changes in its fluorescence emission spectra, shown in Fig.3.1b. The electrostatic potential due to the polymer affects the ionisation of the fluorophore, in line with Equation (3.16). This electrostatic potential is independent of pH, because the acidity constant of the polymer ($pK_A = 4.25$) ensures that PMAA is fully ionized at $pH > 7$. Consequently, the term Δ in Equations (3.16) and (3.19) is constant too, resulting in a constant shift of the effective pK_A of the fluorophore, shown in Fig. 3.2. Computer simulations and fluorescence measurements yield a remarkable agreement, showing that the degree of ionisation is affected by the ionic strength due to screening of the electrostatic interactions by the added salt ions. Interestingly, an attempt to explicitly calculate the “local pH” (local concentration of H^+ ions) and the local electrostatic potential near the fluorophore reveal that the actually measured degree of ionisation is lower than predicted by Equation (3.19). This is caused by temporal fluctuations of the local electrostatic potential due to fluctuating conformation of the polyelectrolyte and by correlation between the conformational fluctuations and fluctuations of the degree of ionisation.[3].

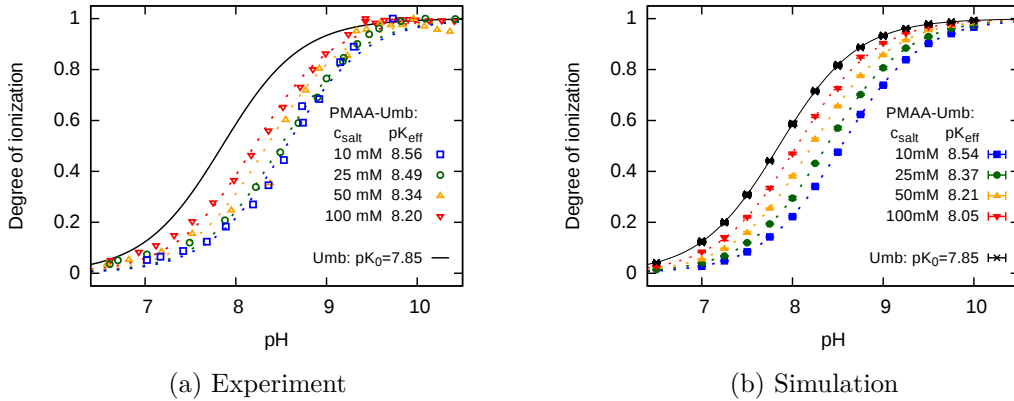


Figure 3.2: Degree of ionisation of Umbelliferone attached to PMAA as a function of pH determined from experiments and simulations at different salt concentrations. Reprinted with permission from Ref.[3]. Copyright (2020) American Chemical Society.

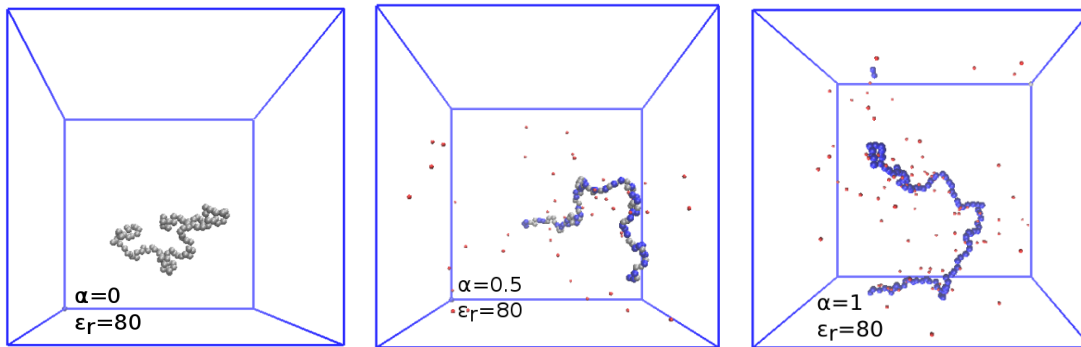


Figure 3.3: Simulation snapshots showing polymer conformations at various degrees of ionization α . From left to right: $\alpha = 0, 0.5$, and 1 . Colour code: silver – uncharged monomer, blue – charged monomer, red – H^+ ion. Reproduced from Ref.[2] with permission from the PCCP Owner Societies.

3.2.3 Ionisation of weak polyelectrolytes

In a weak polyelectrolyte, such as poly(acrylic acid), all monomeric units are ionisable. Consequently, the local electrostatic potential due to ionised groups on a weak polyelectrolyte increases with its degree of ionisation, affecting not only the ionisation states of other ionisable groups but also conformation of the chain, as illustrated in Fig.3.3. Therefore, the relation between ionisation degree of weak polyelectrolytes and pH qualitatively differs from the Henderson-Hasselbalch prediction and cannot be described by a single value of pK_{eff} . The coupling between ionisation and conformation of a weak polyelectrolyte causes that this dependence is less steep than predicted by the Henderson-Hasselbalch equation, as can be seen from Fig.3.4. On the semi-empirical level, these deviations can be described by pK_{eff} that depends on the degree of ionisation, chain length, and on other parameters[10]

$$pK_{\text{eff}}(\alpha, N, c_{\text{pol}}, \dots) = pK_A + \alpha^{1/3} m(N, c_{\text{pol}}, \dots) \quad (3.23)$$

This equation fits the pH-dependent ionisation degree of poly(acrylic acid), however, it fails to fit the ionisation degree of more hydrophobic poly(methacrylic acid). [13] Its practical use rather limited because there is no quantitative theory to predict the dependence of pK_{eff} on system parameters. Nevertheless, its practical implications are

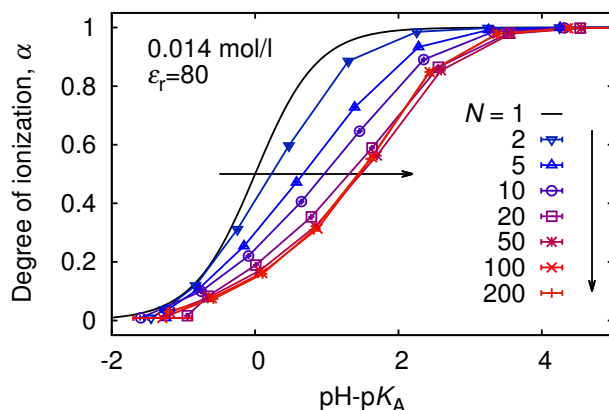


Figure 3.4: Degree of ionisation as a function of pH for polyacids with various numbers of ionisable groups, N , compared to the ionisation of the monomer that follows the Henderson-Hasselbalch equation 3.5. Reproduced from Ref.[2] with permission from the PCCP Owner Societies.

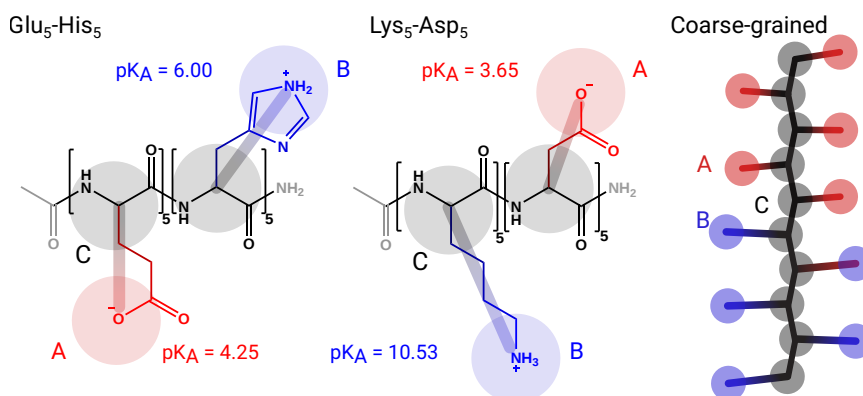


Figure 3.5: Chemical structure of the real peptides and a schematic representation of the coarse-grained bead-spring model consisting of A, B and C beads. Reproduced from Ref.[6] with permission from The Royal Society of Chemistry.

well illustrated by the dependence in Fig.3.4: the deviations significantly increase up to $n \approx 50$ whereas the effect of increasing N becomes barely noticeable beyond this chain length.

3.2.4 Ionisation of weak polyampholytes

The ionisation response of weak polyampholytes is even more complex than that of weak polyelectrolytes composed of only one type of weak acid or weak base groups. In weak polyampholytes, mutual repulsion between like-charged groups (acid or base) suppresses their ionisation, whereas attraction between oppositely charged groups (acid and base) enhances their ionisation. Synthetic peptides can serve as ideal model systems for investigating the pH-responsive properties of ampholytes. Such peptides can be prepared in sufficient purity and with pre-defined sequences that allow us to systematically investigate various combinations of pK_A^{acid} and pK_A^{base} .

To investigate the ionisation response of weak ampholytes, we selected two peptide sequences, each of which was composed of five amino acids with acidic side-chains and five with basic side-chains, shown in Fig. 3.5. By protecting the ionisable groups on the

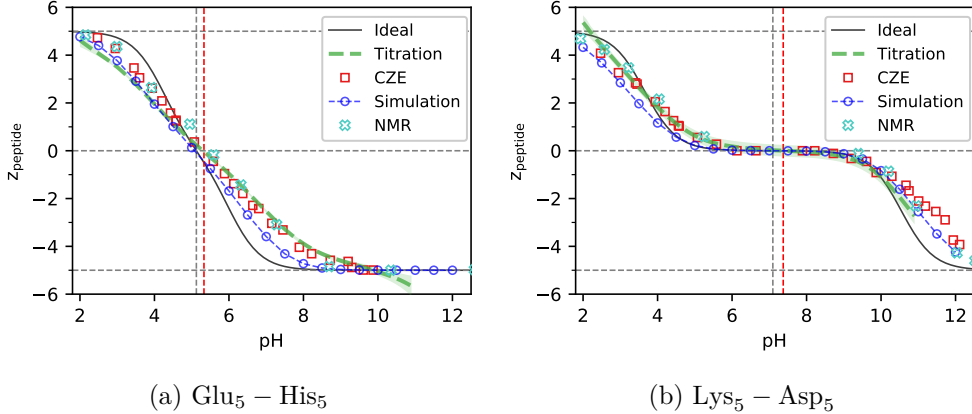


Figure 3.6: Total charge on the peptides as a function of pH from the Henderson-Hasselbalch equation, simulations, NMR, potentiometric titration and capillary zone electrophoresis (CZE). The gray vertical line indicates the ideal isoelectric point whereas the red vertical line indicates the isoelectric point determined from CZE. Reproduced from Ref.[6] with permission from The Royal Society of Chemistry.

C- and *N*-terminus, we obtained a diblock ampholyte with 5 almost equivalent acid groups and the same number of almost equivalent base groups. Such short peptides were molecularly soluble and we were able to determine their charge or ionisation states from coarse-grained simulations and from several independent experimental methods: potentiometric titration, capillary zone electrophoresis (CZE) and nuclear magnetic resonance (NMR), shown in Fig.3.6.

These two peptides differed by $\Delta pK_A = pK_A^{\text{base}} - pK_A^{\text{acid}}$. The Glu₅ – His₅ peptide had $pK_A^{\text{acid}} = 4.25$, $pK_A^{\text{base}} = 6.00$ and a rather small $\Delta pK_A = 1.75$, whereas the Lys₅ – Asp₅ peptide had $pK_A^{\text{acid}} = 3.65$, $pK_A^{\text{base}} = 1.53$ and a much greater $\Delta pK_A = 6.88$. Fig. 3.6 shows that deviations of the ionisation response of these peptides from the Henderson-Hasselbalch equation qualitatively resemble the behaviour of weak polyelectrolytes. As a consequence of the large ΔpK_A , the acid and base groups in the Lys₅ – Asp₅ change their ionisation in two distinct regions of pH. In contrast with that, the small ΔpK_A of the Glu₅ – His₅ peptide implies that both acid and base groups change their ionisation in the same pH range, mutually influencing each other. The relatively short peptide sequences were chosen to ensure that they remain flexible and do not have any well-defined secondary structure. In addition, such short peptides are molecularly soluble and do not aggregate, which facilitates their experimental characterization. By comparing simulation results and experiments in Fig. 3.6, we observed that they agree very well. This agreement demonstrates the power of coarse-grained simulation models in predicting ionisation response of molecules which are much more complex than weak polyelectrolyte homopolymers composed of a high number of identical groups.

Despite very good agreement, a closer inspection of Fig. 3.6 revealed that experimental curves are systematically shifted to a slightly higher pH as compared to the simulation results and to the Henderson-Hasselbalch equation. The origin of this shift is unveiled by comparing the ionisation response of acid and base groups separately, determined from simulations and from NMR experiments. The simulated and experimental curves in Fig. 3.7 consistently show a deformation as compared to the Henderson-Hasselbalch equation. However, some of these curves are systematically shifted with respect to each other. We attributed this shift to the bare pK_A of amino acid side-chains in the peptides being different from the pK_A of the side chains in free amino

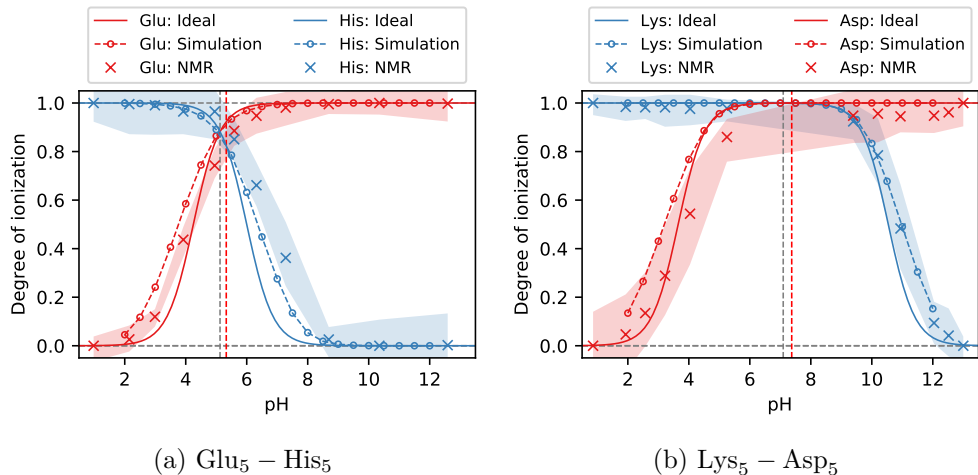
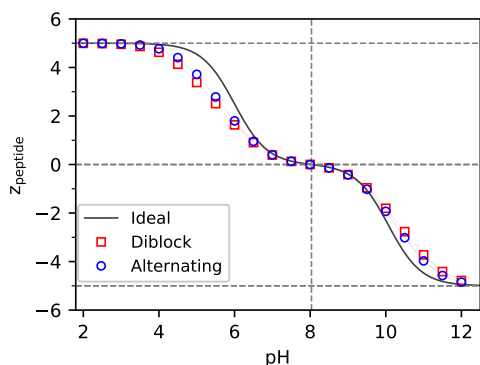


Figure 3.7: The degree of ionisation of acid and base groups on the $\text{Glu}_5 - \text{His}_5$ and $\text{Lys}_5 - \text{Asp}_5$ peptides from simulations, NMR measurements and ideal titration curves. Red and grey vertical lines represent the isoelectric point determined from CZE and from the simulations. Shaded areas indicate the spread of 5 NMR signals corresponding to 5 amino acids of the same type. Reproduced from Ref.[6] with permission from The Royal Society of Chemistry.

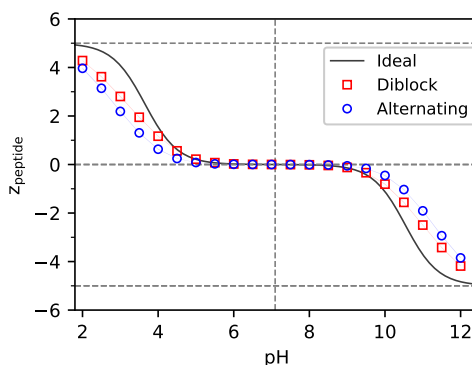
acids.[16] Indeed, the magnitudes of the systematic shifts, observed in Fig. 3.7, decrease with the number of C–C bonds between the peptide bond and the ionisable group on the side-chain. Thus, our analysis reveals that the ionisation response of peptides can be described by two separate effects: (1) effect of local substituents, shifting the $\text{p}K_{\text{A}}$ value as compared to the free amino acid; (2) effect of electrostatic interactions, resulting in a deformation of the ionisation response that cannot be described by using a different $\text{p}K_{\text{A}}$ value but can be described by electrostatic interactions, as revealed by our computer simulations.

Motivated by the success of the combined experimental investigation of the oligopeptides, we performed a systematic study of various oligopeptide sequences with various values of $\Delta\text{p}K_{\text{A}}$, obtained by combining other amino acids with different $\text{p}K_{\text{A}}^{\text{acid}}$ and $\text{p}K_{\text{A}}^{\text{base}}$. It would be rather complicated and expensive to perform such an extensive study experimentally. However, once the model of peptides has been validated, performing such a study by computer simulations was a matter of several weeks.

By comparing the total charge on the peptide as a function of pH, we learned that peptides with positive and negative $\Delta\text{p}K_{\text{A}}$ yield qualitatively very similar deviations from Henderson-Hasselbalch equation, shown in Fig. 3.8. Furthermore, we learned that there is only a small difference between the ionisation response of diblock and alternating sequences, and that this difference almost completely vanishes at $\Delta\text{p}K_{\text{A}} \approx 0$. However, the plot of the degree of ionisation of acid and base groups in Fig. 3.9 reveals that similar deviations of the peptides with positive and negative $\Delta\text{p}K_{\text{A}}$ from Henderson-Hasselbalch equation occur for different reasons. The acid and base groups on peptides composed of Tyr and His are uncharged at the isoelectric point, $\text{pH} \approx \text{p}I$ and their ionisation is lower than predicted by Henderson-Hasselbalch equation as the pH deviates from the $\text{p}I$. In this case, the deviations are caused by electrostatic repulsion between like-charged groups (either acid or base), as in the synthetic polyelectrolytes. On the contrary, the acid and base groups on peptides composed of Lys and Asp are fully ionised at $\text{pH} \approx \text{p}I$ and their ionisation is higher than predicted by Henderson-Hasselbalch equation as the pH deviates from the $\text{p}I$. This increase in ionisation can be explained by electrostatic attraction between oppositely charged groups that pre-

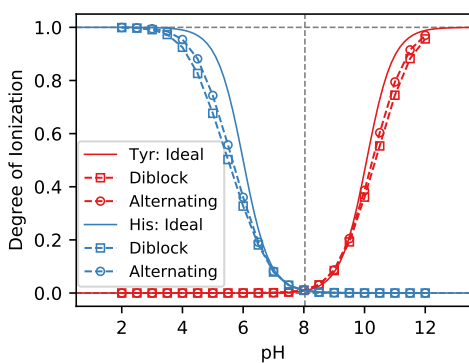


(a) Total charge on diblock Tyr₅ – His₅ and alternating (Tyr – His)₅ peptides with $\Delta pK_A = -4.07$.

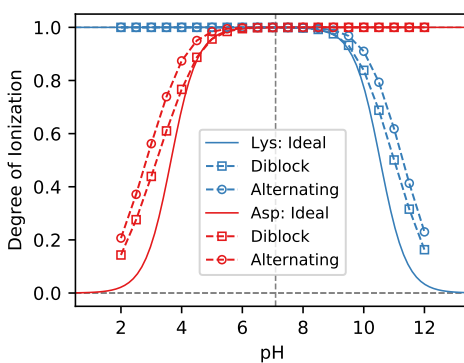


(b) Total charge on diblock Lys₅ – Asp₅ and alternating (Lys – Asp)₅ peptides with $\Delta pK_A = 6.88$.

Figure 3.8: Simulation predictions of the total charge of diblock and alternating peptides with positive and negative ΔpK_A . Solid lines represent the ideal result from the Henderson-Hasselbalch equation. Squares represent the diblock and circles the alternating sequence. Reproduced from Ref.[7].



(a) Degree of ionisation of acid and base groups on Tyr₅ – His₅ and (Tyr – His)₅ with $\Delta pK_A = -4.07$.



(b) Degree of ionisation of acid and base groups on Lys₅ – Asp₅ and (Lys – Asp)₅ with $\Delta pK_A = 6.88$.

Figure 3.9: Simulation predictions of the ionisation degree peptides with positive and negative ΔpK_A . Solid lines represent the ideal result from the Henderson-Hasselbalch equation. Squares represent the diblock and circles the alternating sequence. Reproduced from Ref.[7].

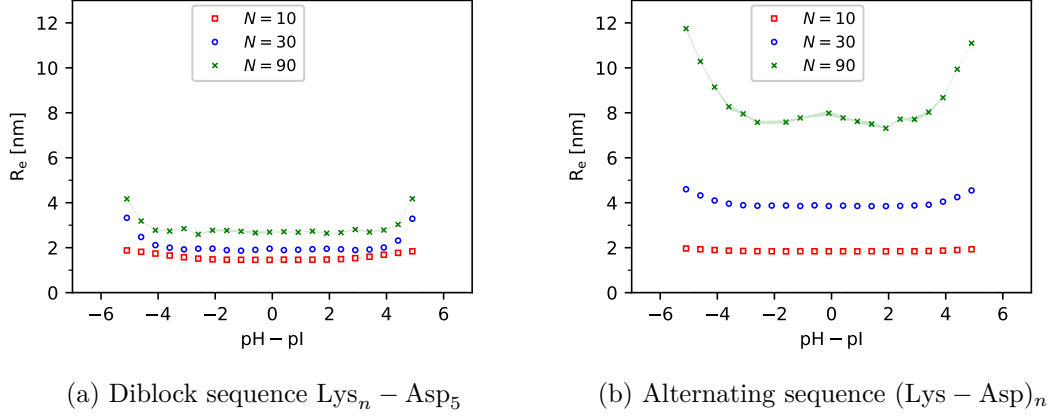


Figure 3.10: Simulation predictions of the end-to-end distances in (a) Diblock peptides $\text{Lys}_n - \text{Asp}_5$ and (b) Alternating peptides $(\text{Lys} - \text{Asp})_n$ with various lengths of the sequences $N = 2n$. Reproduced from Ref.[7].

vails over the repulsion between like-charged groups. However, since the both types of groups are charged at the same time, the total charge on the peptide is determined by the difference between the charge on acid and base groups. Consequently, the charge on peptides with $\Delta\text{p}K_A < 0$ is lower than from the Henderson-Hasselbalch equation because of suppressed ionisation of one type of groups, whereas the charge on peptides with $\Delta\text{p}K_A > 0$ is lower than from the Henderson-Hasselbalch equation because of enhanced ionisation of the other type of groups. The net result is similar for $\Delta\text{p}K_A < 0$ and $\Delta\text{p}K_A > 0$, only as a consequence of mutual cancellation of different effects.

The very small difference between the ionisation response of a diblock and alternating sequences stems from a different cancellation of effects than the similarity of ionisation response at positive and negative $\Delta\text{p}K_A$. Intuitively, one would expect the repulsion between like-charged groups to be stronger in a diblock sequence, whereas like-charge attraction should prevail in the alternating sequence. However, the difference arrangement of groups in these sequences is largely canceled by different conformational changes accompanying the ionisation response. Using the diblock $\text{Lys}_5 - \text{Asp}_5$ and alternating $(\text{Lys} - \text{Asp})_5$ peptides as illustrative examples, Fig. 3.10 shows that the end-to-end distance of both types of sequences attains a minimum as $\text{pH} = \text{pI}$ and maxima at extreme pH values. The diblock sequence is only weakly affected by the pH, whereas the alternating sequence is affected much more, and its end-to-end distance also attains much higher absolute values. Simulation snapshots in Fig. 3.11 illustrate the related conformational changes in $\text{Lys}_5 - \text{Asp}_5$: At the extreme pH values, the charged block is stretched while the other (uncharged) block attains a conformation that resembles a random coil. At $\text{pH} \approx \text{pI}$, the peptide attains a rather compact conformation, resembling a coacervate droplet, because of electrostatic attraction between oppositely charged groups. As expected, these conformational changes become more significant for longer chains because the difference between the random-coil and stretched conformation is smaller if the chains are short.

Simulation predictions from the systematic study of various peptide sequences were only partly validated against experiments.[6] Nevertheless, they provided a basis for the interpretation of pH-responsive behaviour of synthetic polyzwitterions, namely poly(2-(imidazol-1-yl)acrylic acid) (PIAA), poly(dehydroalanine) (PDha), poly(N,N-diallylglutamate) (PDAGA) studied in the group of Prof. F. Schacher at the University of Jena [60], and poly((sulfamate carboxylate) isoprene) (PIS) studied in our group by Dr. M. Uchman and coworkers. [61]

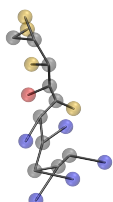
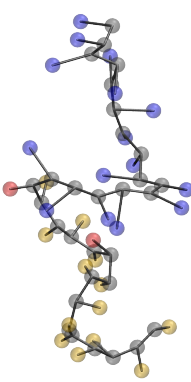
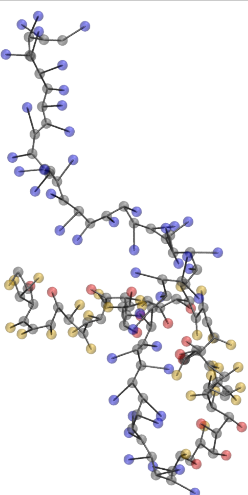
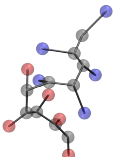
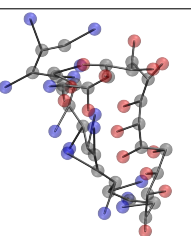
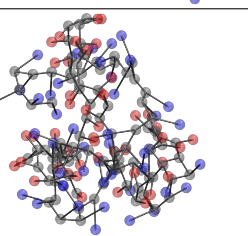
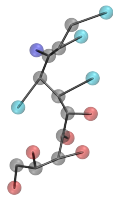
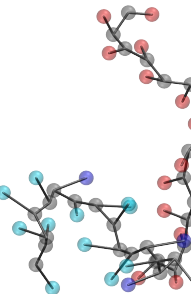
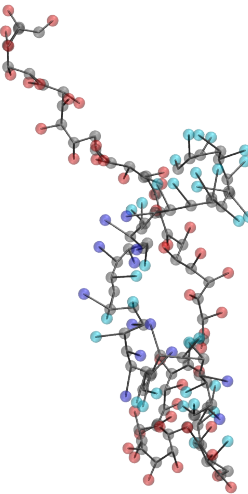
pH	pH - pI	$N = 10$	$N = 30$	$N = 90$
2	$\ll 0$			
7	≈ 0			
12	$\gg 0$			

Figure 3.11: Simulation snapshots of the $\text{Lys}_5 - \text{Asp}_5$ peptide at selected pH values. Colour code: grey = backbone, red = ionised acid group, yellow = non-ionised acid group, blue = ionised base group, cyan = non-ionised base group. Reproduced from Ref.[7].

4. Acid-base equilibria in two-phase systems

Unlike solutions, described in the previous chapter, two-phase systems consist of two parts (phases) that have different macroscopic properties. Nevertheless, these two phases can be in thermodynamic equilibrium and can exchange particles (molecules). The general condition of thermodynamic equilibrium then requires that the chemical potentials of the exchangeable species are identical in both phases, whereas the species that cannot be exchanged can have different chemical potentials in each phase. In this chapter, we will be particularly interested in systems containing polyelectrolytes, coupled to a reservoir that contains only small ions, as illustrated in Fig. 4.1.

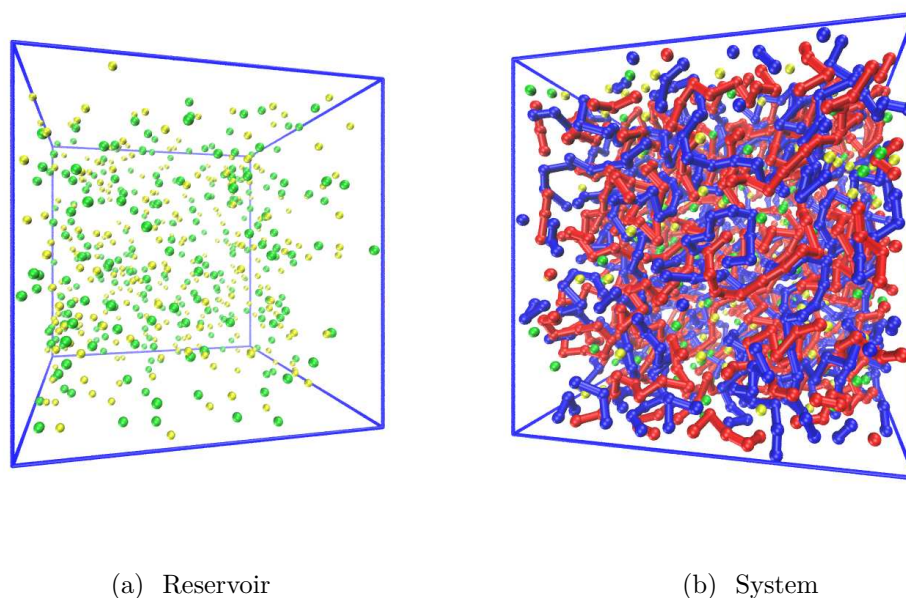


Figure 4.1: Simulation snapshots of a system composed of a coacervate in equilibrium with a reservoir containing only small ions. The small ions can be exchanged between the system and reservoir, whereas polyelectrolytes in the coacervate phase are present only in the system. Figure adopted from Ref.[62] with permission of the author.

Partitioning of ions between two phases can be described using the Donnan equilibrium. The key concept of Donnan equilibrium is the presence of a semipermeable membrane that prevents some ions from entering the other phase, while other ions are free to move between the phases. Typically, the ions that are not allowed to pass to the other side of the membrane are of macromolecular nature: proteins, synthetic polymers, polyelectrolytes, while the small ions are those originating from inorganic salts: Na^+ , Ca^{2+} , Cl^- , SO_4^{2-} , or from the autoprotolysis of water: OH^- , H^+ . Depending on the properties of the membrane, some bigger organic molecules might also be exchanged. An example of such a system could be a solution of proteins or polyelectrolytes in a dialysis bag, immersed in an excess of aqueous solution of sodium chloride. However, there are also membrane-less two-phase systems that exhibit similar features and can be described by the Donnan equilibrium. For example, a polyelectrolyte hydrogel is a three-dimensional crosslinked polymer network in which the ionisable groups are connected to the polymer network by covalent bonds. Therefore, these groups cannot

escape the gel phase, whereas small ions can freely enter and leave, while simultaneously affecting the properties of the gel. Another example of membrane-less systems entails macromolecular solutions that spontaneously phase-separate. For example, mixing of oppositely charged polyelectrolytes often leads to such phase separation, resulting in a polymer-rich liquid coacervate phase in equilibrium with a supernatant solution that does not contain almost any polymer but can exchange small ions with the polymer-rich phase. Because the coacervate phase is usually liquid, this phenomenon is often referred to as liquid-liquid phase separation, that is believed to play an important role in compartmentalization of biological systems containing charged proteins and peptides. Understanding of acid-base equilibria in such two-phase systems is particularly tricky because it entails the complexity of acid-base equilibria of polyelectrolytes, discussed in the previous chapter, that is further complicated by the partitioning of low-molecular species that affect the properties of both phases.

4.1 The Donnan equilibrium

The Donnan equilibrium is often described in the literature as an electrostatic potential difference that the ions need to overcome in order to pass to the other side of the membrane. While this picture is realistic, it can be simultaneously misleading because it hides the key assumptions made in the derivation of the well-established Donnan formula.

The key assumption used in deriving the Donnan equilibrium is that systems on both sides of the membrane are electroneutral. Next, it is assumed that the ions are not interacting with each other, i.e., they behave as an ideal gas. By requiring that the chemical potential of each ionic species is the same on each side of the membrane, the electroneutrality condition can be simultaneously satisfied only with an additional assumption of a potential ψ associated with crossing the barrier by an ion of type i and valency z_i :

$$c_i^I = c_i^{II} e^{z_i \psi} \quad (4.1)$$

where labels I and II refer to different phases. Although Equation 4.1 can be derived in a mathematically straightforward way, it has one conceptual problem: If we impose the constraint of electroneutrality, then it is not possible to remove a single ion from any of the phases, and therefore a chemical potential of single ion is ill-defined. With the electroneutrality constraint, it is only possible to define the chemical potential of a pair of monovalent ions, or more generally an electroneutral group of ions that could be simultaneously exchanged between the phases. While this conceptual problem seems to be academic, it has significant impact on simulations of thermodynamic equilibria that involve the Donnan partitioning of ions. In simulations, the numbers of ions are typically low, and removing or inserting one ion can significantly violate electroneutrality of the simulated system.

We note that electroneutrality is not strictly obeyed in real systems. It can be locally violated at the nanoscale, so that individual ions can be exchanged between macroscopic phases. Such an exchange of ions indeed leads to a build-up of electrostatic potential across the interface, that prevents further ions from passing to the other side. From this perspective, the electroneutrality constraint and Donnan potential are just convenient approximations that allow us to describe the properties of macroscopic phases while avoiding a detailed description of the structure of their interface.

When simulating phase equilibria, however, we strictly require that electroneutrality of the simulation box is conserved. In such case, electroneutrality becomes a constraint that needs to be handled in a conceptually consistent way. We showed that this can be done when deriving the Donnan equilibrium in an ideal-gas system by minimizing the

total free energy of both phases (I and II), while simultaneously satisfying the electroneutrality constraint. By this procedure, the Donnan potential is obtained as an additional contribution to the chemical potential, originating from a Lagrange multiplier from the constrained minimization. It possesses the same symmetry with respect to the valency of ions as the electrostatic potential, however, its origin is different. It is particularly important when considering Donnan equilibria in systems with electrostatic interactions while using the electroneutrality constraint instead of explicitly describing the interface. In such case, the Donnan potential needs to be distinguished from the actual electrostatic potential that arises from interactions between the ions.

Donnan Contribution to the Chemical Potential

We define the extended chemical potential μ of species i as a sum of the reference, ideal, excess and Donnan contributions,

$$\mu_i = \mu_i^\ominus + \mu_i^{\text{id}} + \mu_i^{\text{ex}} + z_i \mu^{\text{don}} \quad (4.2)$$

where z_i is the valency of species i . We choose the convention that the reference chemical potential μ^\ominus is the chemical potential of an ideal gas at reference concentration $c^\ominus = 1$ M. The ideal contribution μ_i^{id} is defined as

$$\mu_i^{\text{id}} = k_{\text{B}}T \ln(c_i/c^\ominus) \quad (4.3)$$

where c_i is the concentration of species i . The excess contribution μ_i^{ex} arises from direct intermolecular interactions, therefore $\mu^{\text{ex}} = 0$ for a non-interacting system. The Donnan contribution μ^{don} arises from minimizing the total free energy of (system + reservoir) under the electroneutrality constraint, using the convention that $\mu^{\text{don}} = 0$ in the reservoir. Unlike all other contributions to the chemical potential, the term μ^{don} is the same for all ions, however, it contributes differently the chemical potentials of various ions, because it is multiplied by their valency. Therefore, it follows from Eq.4.2 that the Donnan potential exactly cancels for any group of exchangeable ions that is overall electroneutral

$$\sum_i z_i \mu^{\text{don}} = \mu^{\text{don}} \sum_i z_i = 0 \quad (4.4)$$

With the definition in (4.2), the extended chemical potentials are equal in the system and in the reservoir. We use the term extended to emphasize that our definition of the chemical potential includes the Donnan term, which is usually omitted. This term must be accounted for when considering chemical reactions inside the system, involving constituents exchanged with the reservoir. The μ^{don} term leads to a partitioning of ions between the system and the reservoir, that is commonly known as the Donnan partitioning[63, 64, 65].

The activity, a , can be defined in analogy with (4.3), as:

$$\mu_i^{\text{id}} + \mu_i^{\text{ex}} = k_{\text{B}}T \ln a_i \quad (4.5)$$

which is also used in the IUPAC definition of pH[56], given in (3.12). A measurement of pH in the system actually yields the activity of an ion pair[66] because the activity of a single ion cannot be measured. When measuring the chemical potential of an ion pair, the Donnan contributions of both ions cancel each. Therefore, the definition of activity does not include the Donnan potential, and the values of pH measured in the system and in the reservoir differ by the Donnan term:

$$\text{pH}_{\text{sys}} = \text{pH}_{\text{res}} + \frac{\mu^{\text{don}}}{k_{\text{B}}T \ln(10)} \quad (4.6)$$

Equation (4.6) shows that a negative value of μ^{don} implies $\text{pH}_{\text{sys}} < \text{pH}_{\text{res}}$, and a positive value of μ^{don} implies $\text{pH}_{\text{sys}} > \text{pH}_{\text{res}}$. Because pH in the reservoir is usually the parameter that is controlled directly, we introduce the convention that from now on pH without superscript always denotes the pH measured in the reservoir. However, we keep the subscript whenever it is necessary to distinguish the two contributions in one equation.

Donnan equilibrium involving multiple ionic species

The partition coefficient ξ_i of an ionic species i is defined as the ratio of its concentrations in the system and in the reservoir

$$\xi_i = \frac{c_i^{\text{sys}}}{c_i^{\text{res}}} = \exp\left(-\frac{z_i \mu^{\text{don}}}{k_B T}\right) \quad (4.7)$$

If the anions A^- are the only species that cannot be exchanged between the system and the reservoir, then the partition coefficient can be expressed as

$$\xi_i = \frac{c_i^{\text{sys}}}{c_i^{\text{res}}} = \frac{z_i c_{A^-}}{2I^{\text{res}}} + \sqrt{\left(\frac{c_{A^-}}{2I^{\text{res}}}\right)^2 + 1} \quad (4.8)$$

where I^{res} denotes the ionic strength in the reservoir, defined as

$$I^{\text{res}} = \frac{1}{2} \sum_i z_i^2 c_i^{\text{res}} \quad (4.9)$$

We use the same formula to define the ionic strength in the system, but in this case the summation runs only over exchangeable ions, excluding the charges on the polyelectrolyte.

4.1.1 Effect of electrostatics on the Donnan partitioning

It is possible to cast the Donnan partitioning in the form of a universal master curve, that is independent of the valency of ions and the ionic strength [5]

$$\xi_i - (z_i - z_{A^-}) c_{A^-}^{\text{sys}} / 2I^{\text{res}} = \begin{cases} \xi_i, & \text{coions} \\ \xi_i - c_{A^-}^{\text{sys}} / I^{\text{res}}, & \text{counterions} \end{cases} \quad (4.10)$$

where z_i is the valency of ion i ($z_{\text{H}^+} = z_{\text{Na}^+} = +1$; $z_{A^-} = z_{\text{Cl}^-} = z_{\text{OH}^-} = -1$). Fig.4.2(a) shows that the results of our simulations of various non-interacting systems coincide with this master curve at all ionic strengths, pH values and concentrations of non-exchangeable ions. Fig.4.2(b) shows that this the simulation results for interacting systems deviate from this universal description. In such case, deviations from the master curve can be seen as a measure of the effect of interactions on the partitioning of small ions at specific conditions (pH, ionic strength, concentration of non-exchanged ions). As we have shown in Ref.[5], these deviations predominantly originate from electrostatic interactions, whereas steric effects contribute only at high concentrations. However, hydrophobicity or other type of specific short-ranged interactions may contribute significantly even at rather low concentrations, as we have shown in a related study of polyelectrolyte micelles interacting with hydrophobic counterions.[67]

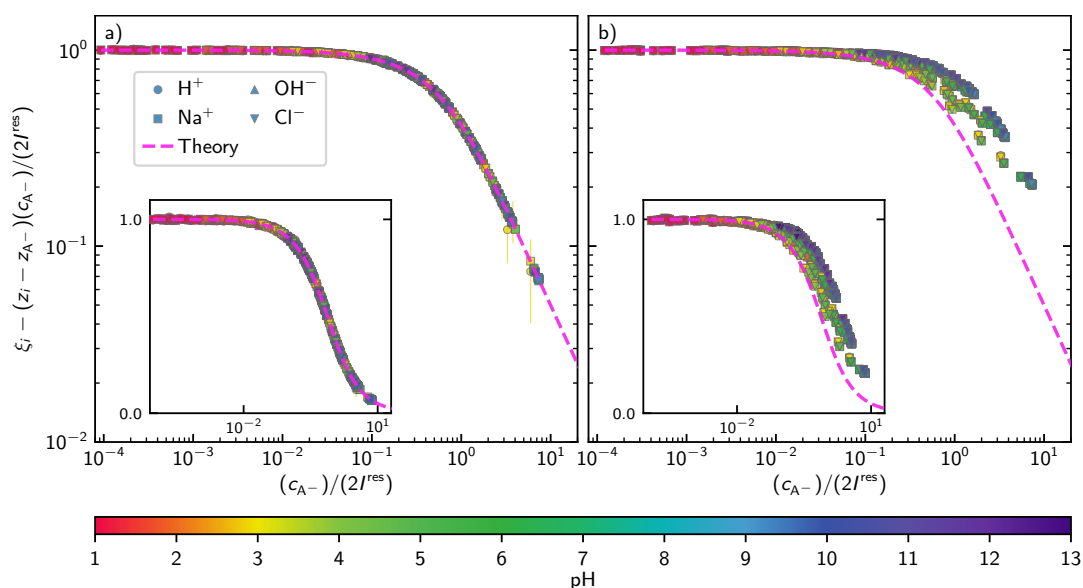


Figure 4.2: Ion partitioning predicted by the Donnan theory[63, 65], compared with simulation results from the Grand-reaction method. The pink dashed line represents the generalized Donnan prediction. Partitioning of various ions from the simulations is encoded by different symbol shapes, as indicated in the legend. The color code indicates the reservoir pH in each simulation. Panel (a) shows the partitioning in an ideal system *without* interactions. Panel (b) shows the partitioning in a polymer solution *with* interactions. Reprinted with permission from Ref.[5]. Copyright (2020) American Chemical Society.

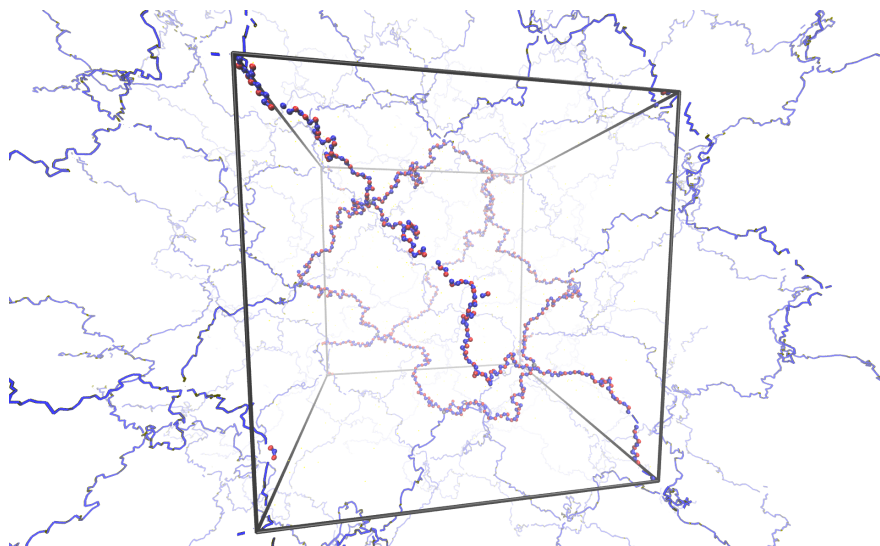


Figure 4.3: Simulation snapshot of a swollen polyelectrolyte hydrogel network. The cube denotes the actual simulation box. Periodic images of the gel are included to illustrate the quasi-infinite network. Reprinted with permission from Ref.[1]. Copyright (2020) American Chemical Society.

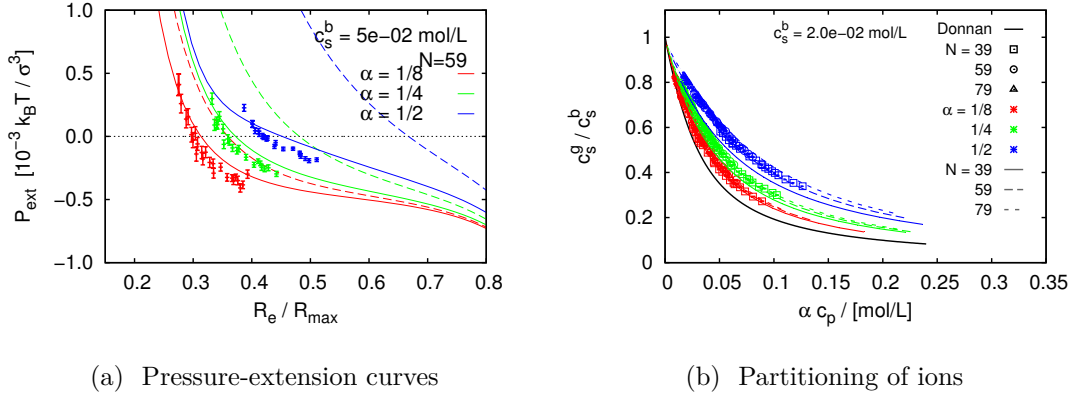


Figure 4.4: The balance of pressures (left) and Donnan partitioning of small ions (right) determine the swelling equilibrium of polyelectrolyte hydrogels. Both figures compare simulation results (points) and theoretical prediction (lines of the matching colour) for hydrogels at selected parameters: chain length N , degree of ionisation α and salt concentration in the reservoir, $c_{\text{salt}}^{\text{res}}$. Reprinted with permission from Ref.[1]. Copyright (2020) American Chemical Society.

4.1.2 Polyelectrolyte hydrogels in salt solution

The Donnan partitioning and electrostatic interactions are the key parameters that determine the swelling of polyelectrolyte hydrogels in aqueous solutions. Their swelling can be qualitatively explained using the Flory-Rehner theory[68]. The Donnan partitioning of ions causes a difference in osmotic pressures between the system (gel) and the reservoir (salt solution) that in turn causes swelling of the gel. This swelling is opposed by a contribution to pressure that originates from the entropy loss due to stretching of the chains inside the network. In the simplest case, if we neglect all other contributions, then the free swelling equilibrium is achieved when these two contributions are balanced, resulting in zero net pressure acting on the gel, $P_{\text{ext}} = 0$. In Fig.4.4a we illustrate how this pressure balance can be used to determine the chain extension, R_e , that corresponds to the free swelling equilibrium. The chain extension determines the concentration of ionised groups inside the gel, that in turn determines the Donnan partitioning of small ions. This partitioning is presented in Fig.4.4b as the ratio of salt concentration in the gel and in the reservoir $c_{\text{salt}}^{\text{gel}} / c_{\text{salt}}^{\text{res}}$. The simulation data qualitatively follows the trend predicted by the Donnan theory. However, Fig.4.4b shows that then Donnan theory predicts lower salt concentrations in the gel than observed in the simulations. These simulation results are well represented by the augmented theory of ion partitioning due to Katchalsky and Michaeli[10], shown as dashed lines in Fig.4.4b.

By obtaining a set of pressure-extension curves at various conditions, it is possible to predict how the swelling ratio of the gel depends on the salt concentration in the reservoir, and also on the gel parameters: ionisation degree α and chain length N . In experiments, the swelling ratio is usually defined as the ratio of volumes of the swollen and dry gel $Q_{\text{exp}} = V / V_{\text{dry}}$. For polyelectrolyte gels, it can attain values on the order of $Q \approx 10^3$ in low-salt conditions, and $Q \approx 10^2$ at moderate salt concentrations. In modeling, it is more practical to define the swelling ratio as volume of the swollen gel divided by the volume of an ideal neutral gel, $Q = V / V_{\text{id}}$. Therefore, Q from the simulations follows the same trend but attains much lower values, because it is normalized by a different constant $V_{\text{id}} \gg V_{\text{dry}}$. Nevertheless, this different normalization constant has no effect on the overall trend of the curves. It just affects the numerical values of Q .

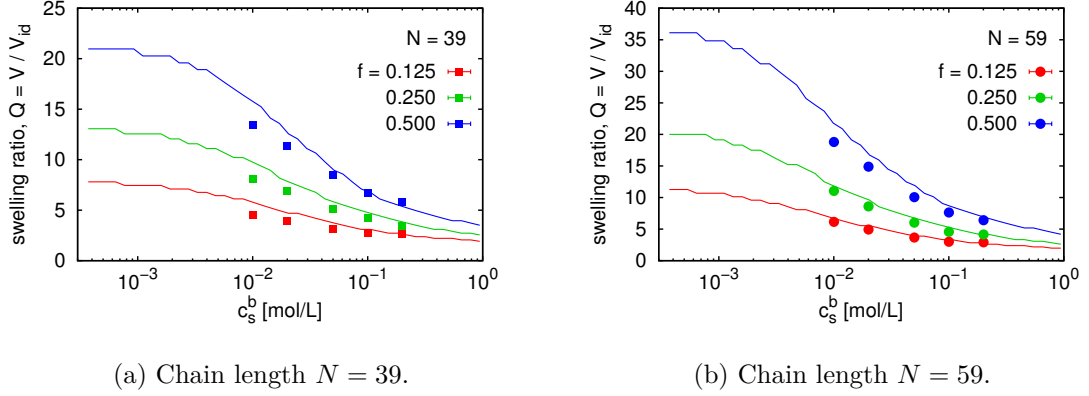


Figure 4.5: The swelling ratio of polyelectrolyte hydrogels as a function of salt concentration. Reprinted with permission from Ref.[1]. Copyright (2020) American Chemical Society.

Fig.4.5 shows that the swelling of polyelectrolyte hydrogels decreases with increasing salt concentration, and that the hydrogels swell more if they have a higher degree of ionisation (α) or lower density of cross-linking (higher N). The solid lines in Fig.4.5 show that this swelling reaches a saturation value at low salt. At high degree of ionisation, this saturation is determined by the maximum stretching of the gel strands of chain length N .

All simulations discussed in this section used the degree of ionisation as a fixed input parameter of the simulation. However, many polyelectrolyte hydrogels are based on weak polyelectrolytes, such as poly(acrylic acid) with $pK_A = 4.25$. The ionisation degree of these hydrogels depends on pH of the solution. Furthermore, it depends on the Donnan potential, because the H^+ ions are subject to Donnan partitioning. The Donnan partitioning depends on the swelling ratio of the gel, that in turn depends on the ionisation degree, creating a complicated feedback loop. Therefore, predicting the ionisation and swelling of weak polyelectrolyte hydrogels is a challenge for theory and simulations. At present, we have such predictions available, however, they have not been published yet. Therefore, we did not include them in this thesis. Instead, we illustrate the related physico-chemical concepts on a simple system of a weak polyelectrolyte solution coupled to a reservoir at a given pH and ionic strength.

4.2 Acid-base equilibrium coupled to a reservoir

Consider a general chemical reaction, defined by the stoichiometry:



where ν_A is the stoichiometric coefficient of species A, and analogously for all other species. Equation 4.11 can be rewritten as $\sum_i \nu_i X_i = 0$, which uses the convention that $\nu < 0$ for the reactants (species on the left-hand side of (4.11)) and $\nu > 0$ for products (species on the right-hand side of (4.11)). The corresponding equilibrium constant is defined as

$$k_B T \ln K = - \sum_i \nu_i \mu_i^\ominus \quad (4.12)$$

Chemical equilibrium requires that $\sum_i \nu_i \mu_i = 0$, which allows us to express K as

$$k_B T \ln K = \sum_i \nu_i (\mu_i - \mu_i^\ominus) = \sum_i \nu_i (\mu_i^{\text{id}} + \mu_i^{\text{ex}} + z_i \mu^{\text{don}}) \quad (4.13)$$

If we require that the reaction is overall electroneutral, $\sum_i \nu_i z_i = 0$, then the Donnan contributions in (4.13) exactly cancel each other. Therefore, the reaction equilibrium in the system depends only on concentrations of individual species in the system but it does not explicitly depend on the Donnan potential. However, the Donnan potential affects the partitioning of all exchangeable ions, and therefore it affects their concentrations in the system. This change in composition then affects the chemical equilibrium of reactions in which some ionic species cannot be exchanged. When applying these considerations to the ionisation reaction of a weak acid (2.1), we can express the Henderson-Hasselbalch equation in terms of pH in the system or pH in the reservoir

$$\text{pH}_{\text{sys}} - \text{p}K_{\text{A}} \stackrel{\text{ideal}}{=} \log_{10} \left(\frac{\alpha}{1 - \alpha} \right) \quad (4.14)$$

$$\text{pH}_{\text{res}} - \text{p}K_{\text{A}} \stackrel{\text{ideal}}{=} \log_{10} \left(\frac{\alpha}{1 - \alpha} \right) - \frac{\mu^{\text{don}}(\alpha)}{k_{\text{B}}T \ln(10)} \quad (4.15)$$

where $\alpha = c_{\text{A}^-} / (c_{\text{A}^-} + c_{\text{HA}})$ is the ionisation degree of the acid. By writing $\mu^{\text{don}}(\alpha)$, we emphasize that the Donnan contribution depends on α . Equations (4.7) and (4.8) imply that if the non-exchanged species is an anion A^- , then $\mu^{\text{don}} < 0$ and $\text{pH}_{\text{sys}} < \text{pH}_{\text{res}}$. Therefore, the Donnan partitioning decreases the ionisation of the weak acid in the system in comparison with the ionisation in the reservoir. Conversely, if the non-exchanged species is a weak base, then $\mu^{\text{don}} > 0$ and $\text{pH}_{\text{sys}} > \text{pH}_{\text{res}}$, in this case decreasing ionisation of the weak base. If the non-exchanged species include both positively and negatively charged groups, then the Donnan potential can have different signs, depending on the valency of the groups that are in excess. In such a case, the Donnan partitioning may also result in an increased ionisation, as we illustrate in Section 4.2.2. In an ideal non-interacting system, only the Donnan contribution shifts the ionisation equilibrium. In an interacting system, both ionisation equilibrium and Donnan partitioning are affected by the interactions, which can be evaluated in a computer simulation.

Extension to non-ideal systems

All the above considerations can be easily extended to non-ideal interacting systems by explicitly accounting for inter-particle interactions, which only affect the excess chemical potentials but do not affect the Donnan potential. The excess chemical potentials are non-zero in an interacting system, and they do not cancel for oppositely charged ions. Conversely, they tend to have the same sign and they also have the same magnitude if the system is symmetric with respect to the sign of all charges. In contrast with that, the Donnan contribution is non-zero in an ideal system and it exactly cancels for any electroneutral group of ions.

4.2.1 Weak polyacid coupled to a reservoir

To illustrate how the acid-base equilibrium is affected by the Donnan partitioning, let us consider a weak polyacid in a dialysis bag, in contact with an external reservoir at a given pH and concentration of salt ions ($\text{pH}_{\text{res}}, c_{\text{salt}}^{\text{res}}$). Ionisation of the polyacid is suppressed as compared to the monomeric acid because of like-charge repulsion between ionisable groups on the backbone. This effect is well known from the discussion of polyelectrolyte solutions in Section 3, therefore, we call it the *polyelectrolyte effect*. In addition, the ionisation is further suppressed as a consequence of Donnan partitioning of H^+ ions, that we call the *Donnan effect*. The role of these two effects is demonstrated in Fig.4.6 by comparing the Henderson-Hasselbalch (HH) prediction with two simulation methods. The grand-reaction method (G-RxMC) accounts for both effects, resulting in

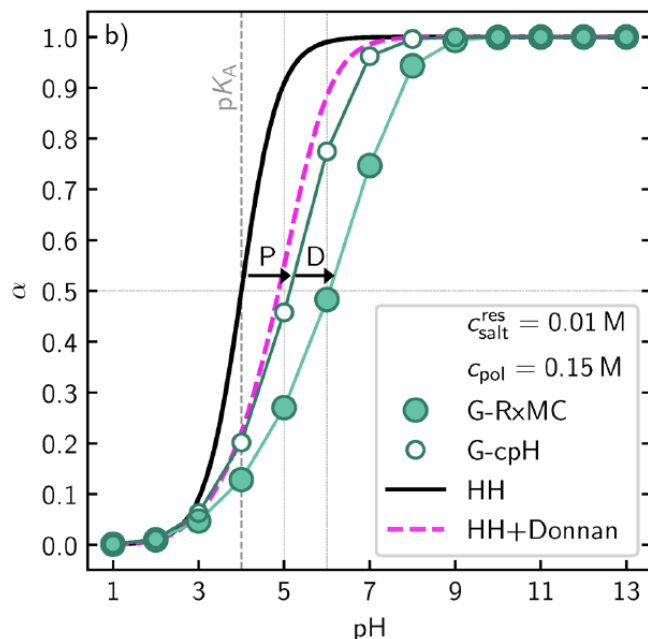


Figure 4.6: Ionisation degree as a function of reservoir pH, comparing different methods. Vertical and horizontal lines are guides to help estimating the magnitude of the Donnan and the polyelectrolyte effect at $\alpha = 0.5$. Arrows indicate the magnitude of the polyelectrolyte effect “P”, and the Donnan effect “D”. Reprinted with permission from Ref.[5]. Copyright (2020) American Chemical Society.

a shift of the ionisation by about two units of pH towards higher pH values. In contrast, the grand-constant-pH method (G-cpH) accounts for the electrostatic interactions but it assumes that pH in the system is the same as in the reservoir, neglecting the Donnan contribution to the pH. The shift predicted by the G-cpH method amounts to roughly one half of the full shift predicted by the G-RxMC method. By combining the Henderson-Hasselbalch equation with the Donnan partitioning (HH+Donnan), we account for the Donnan contribution to the pH, but neglect the direct contribution of electrostatic interactions. Interestingly, the HH+Donnan prediction in Fig.4.6 is very similar to the G-cpH prediction, demonstrating that the polyelectrolyte effect and Donnan effect can be comparably strong. The G-RxMC method, introduced by ourselves [5], was presumably the first simulation method that treats both these effects on equal footing.

Depending on the conditions, either Polyelectrolyte or Donnan effect can dominate, or their magnitude can be comparable. This is important when discussing the swelling of weak polyelectrolytes in solution or weak polyelectrolyte gels as a function of pH. Fig.4.7(a) shows that the polyelectrolyte effect dominates at low concentration of ionisable groups on the polymer. Therefore, the degree of ionisation only very weakly depends on the salt concentration. Fig.4.7(b) shows that the chain swelling as a function of pH follows the same trend for both salt concentrations, however, it reaches a higher value at lower salt. In contrast, Fig.4.7(c) shows that the relative importance of the polyelectrolyte and Donnan effects varies if we compare different polymer concentrations at the same salt concentration. In both cases, the degree of ionisation as a function of pH follows the same trend. However, as can be seen by comparing with the G-cpH predictions in the same figure, this trend is dominated by the polyelectrolyte effect at low polymer concentration, whereas both effects contribute comparable at a higher polymer concentration. Interestingly, even though the ionisation degree as a function of pH in Fig.4.7(c) is the same for both polymer concentrations, the chain

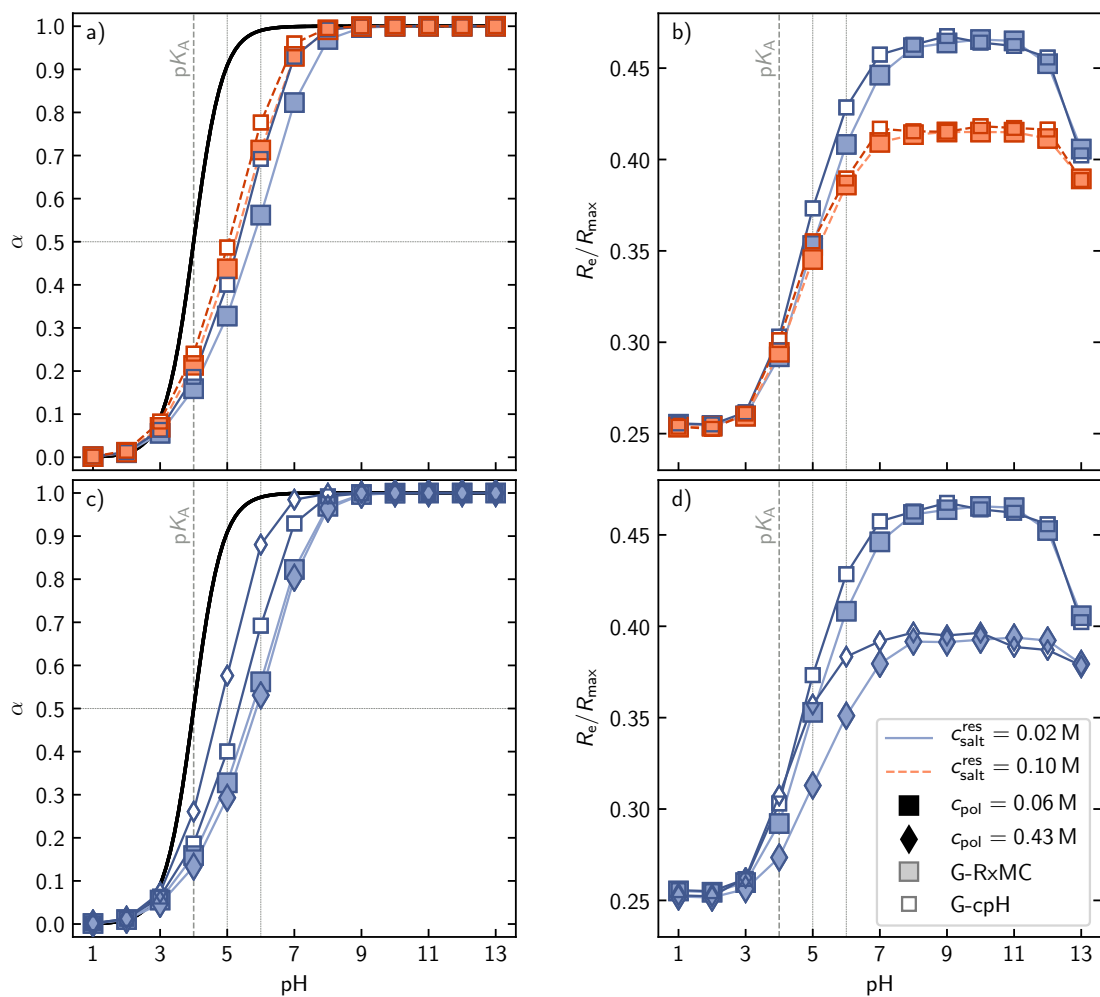


Figure 4.7: Degree of ionisation (a + c) and end-to-end distance (b + d) of the weak polyelectrolyte chain with $pK_A = 4.0$ as a function of the reservoir pH. To differentiate the polyelectrolyte effect from the Donnan effect, we compare G-RxMC and G-cpH simulations. Vertical and horizontal lines are guides to help estimating the magnitude of the Donnan and the polyelectrolyte effect at $\alpha = 0.5$. Reprinted with permission from Ref.[5]. Copyright (2020) American Chemical Society.

swelling as a function of pH in Fig.4.7(d) exhibits a different trend. This difference can be attributed to a competition between direct electrostatic repulsion between like charges on the chain and electrostatic screening due to the different spatial distribution small ions in these systems.

4.2.2 pH-controlled phase separation

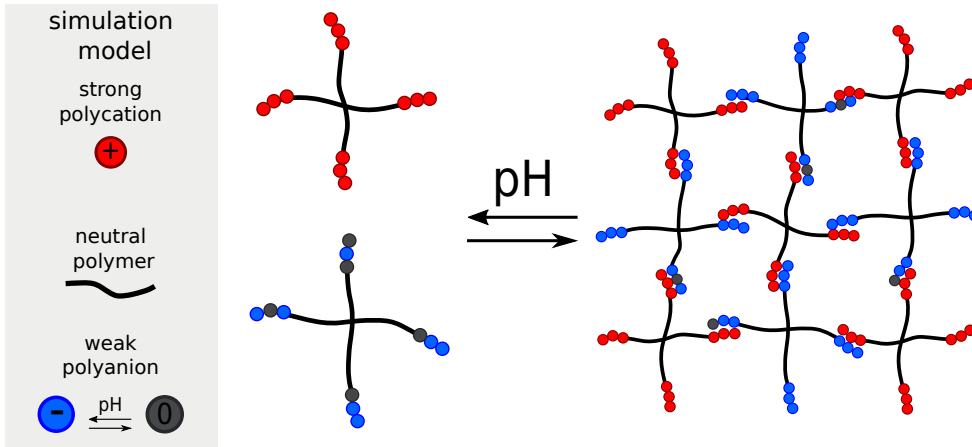


Figure 4.8: Schematic representation of the formation of electrostatically crosslinked gel of star polymers with oppositely charged polyelectrolyte blocks. Reprinted with permission from Ref.[8]. Copyright (2021) American Chemical Society.

Mixing of neutral polymers terminated by oppositely charged polyelectrolyte blocks results in the formation of a polymer-rich phase in equilibrium with a supernatant solution that contains salt ions but no polymer. Oppositely charged blocks in the polymer-rich phase form nano-domains, interconnected by blocks composed of neutral monomers, resulting in the formation of an electrostatically crosslinked polyelectrolyte gel, illustrated in Fig.4.8. Unlike covalently crosslinked polyelectrolyte gels, discussed in preceding sections, electrostatically crosslinked gels can be reversibly assembled and disassembled upon a change in the external conditions – salt concentration or pH.

To investigate this reversible gelation in simulations, we employed a similar approach as in the case of covalently crosslinked polyelectrolyte gels. We simulated a system of star polymers whose arms were terminated by strong polycationic end blocks, mixed with a stoichiometric equivalent of star polymers whose arms were terminated by weak polyanionic end block with $pK_A = 9.87$. By simulating this system at different polymer concentrations, coupled to a reservoir at a given salt concentration and pH, we determined at which conditions the system and the reservoir were at equal pressures. At high salt concentrations, the balance of pressures was not achieved, indicating that a single phase (homogeneous solution) was thermodynamically stable. At low salt concentrations, the polymer-rich phase is in equilibrium with supernatant phase, resulting in a sol (dispersion of small clusters of stars) at $pH \approx pK_A$ or a gel (infinite network of stars) at a slightly higher pH. This reversible assembly and disassembly is illustrated by the simulation snapshots in Fig.4.9. At $pH_{res} \approx 10.0$, this system forms cluster consisting of a small number of oppositely charged stars, whereas at $pH_{res} \approx 11.9$ the same system forms an interconnected network – a gel of stars.

Fig.4.10 shows that the degree of ionisation of the weak acid groups in the gel composed of stars follows the ideal Henderson-Hasselbalch equation. In contrast with that, degree of ionisation of the same stars is strongly suppressed in a dilute solution, in the absence of their oppositely charged counterparts. Thus, we observe that mixing

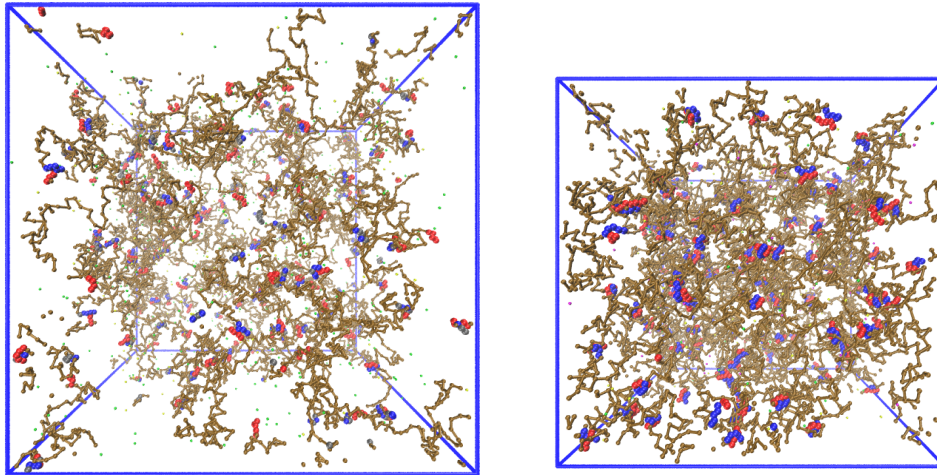


Figure 4.9: Snapshots of the polymer-rich phase in equilibrium with the reservoir at: $\text{pH}^{\text{res}} \approx 10.0$ (resulting in $c_{\text{pol}} \approx 0.5 \text{ mM}$) on the left, and $\text{pH}^{\text{res}} \approx 11.9$ (resulting in $c_{\text{pol}} \approx 1.7 \text{ mM}$) on the right. Color code: blue – ionised anionic segments A^- , gray – neutral anionic segments HA , red – cationic segments B^+ , brown – neutral segments, yellow – Na^+ ions, green – Cl^- ions, magenta – OH^- ions. Reprinted with permission from Ref.[8]. Copyright (2021) American Chemical Society.

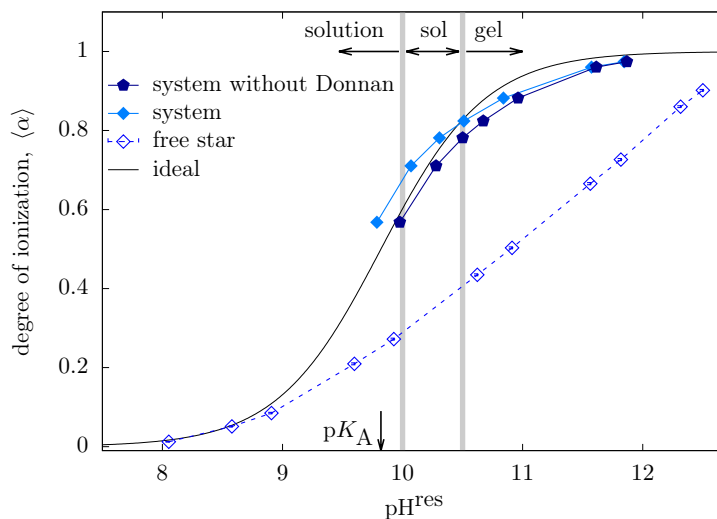


Figure 4.10: Titration curve of positively charged stars in the gel compared to the same star in a dilute solution at $I \approx 13.2 \text{ mM}$ and $c_{\text{mon.}} \approx 33.5 \text{ mM}$. These curves are also compared to the ideal titration curve and to a titration curve explicitly excluding the Donnan effect on pH. The vertical lines mark the estimated pH thresholds for the phase separation and sol-gel transition. Reprinted with permission from Ref.[8]. Copyright (2021) American Chemical Society.

with oppositely charged stars enhances the ionisation of the weak polyanions, enabling the pH-triggered gelation at pH values, at which isolated stars in solution would not be sufficiently ionised to form a gel. This cooperativity of ionisation upon mixing of cationic and anionic groups in the same system is analogous with the cooperativity observed in the ionisation of weak ampholytes. However, unlike weak ampholytes, oppositely charged groups in the gel of stars belong to different molecules, and their cooperative response to pH takes place only if these molecules are mixed together.

5. Conclusions and outlook

We have presented an overview of computer simulations and experimental results that shed some light on the complexity of acid-base equilibria in charged macromolecular systems. We have obtained a detailed mechanistic understanding of how the interactions between like-charged and oppositely charged ionizable groups affect the acid-base properties of weak polyelectrolytes and weak polyampholytes. We have developed a simulation method that allowed us to investigate how the Donnan partitioning of small ions, and especially H^+ ions, affects these equilibria in two-phase systems, consisting of a polymer-rich phase, and a supernatant solution.

The research that we have conducted in the last 10-15 years will continue along two lines. In the first line, we plan to systematically develop fundamental studies of model systems, gaining deeper mechanistic insights and answering some questions that have remained unanswered in our previous work. These studies will include systematic more complex ampholytes, such as polyzwitterions, synthesized by our collaborators within the Soft Matter research group in Prague, or external collaborators at the university of Jena. We plan to further develop the simulation methods for two-phase systems, furthering our collaboration with the prof. C. Holm at the University of Stuttgart, or to develop coarse-grained models to predict acid-base properties of model proteins. Before that, We will extend the existing investigations of model oligopeptides by considering more complicated sequences of acidic, basic and neutral (hydrophobic or hydrophilic) amino acids. The second line consists of applying the gained knowledge to explain specific experimental observations, or using simulation predictions to guide experimental design of specific systems. Simulations and experimental investigations of diblock ampholytic peptides interacting with various polyelectrolytes are in progress, in collaboration with colleagues within the soft-matter group, or at the institute of macromolecular chemistry of the Czech Academy of Sciences. Recently, experimental research in the Soft Matter group has focused on pH-responsive polymer systems based on boronic acids, and we are working on a modification of the RxMC method in order to account for several competing acid-base equilibria and association reactions in these systems. The grand-reaction method provides new possibilities of investigating two-phase systems that include the swelling of weak polyelectrolyte hydrogels, stability of complex coacervates, or aggregation of proteins, and partitioning of small ionic species in these phase-separated systems. Last but not least, it should be mentioned that the grand-reaction method seems to be suitable for modeling the ionization states of redox-active polymers used in redox-flow batteries.

Included publications

- [1] Peter **Košovan**, Tobias Richter, and Christian Holm. Modelling of polyelectrolyte gels in equilibrium with salt solutions. *Macromolecules*, 48:7698–7708, 2015.
- [2] Lucie Nová, Filip Uhlík, and Peter **Košovan**. Local pH and effective pK_A of weak polyelectrolytes - insights from computer simulations. *Phys. Chem. Chem. Phys.*, 19:14376–14387, 2017.
- [3] Anastasiia Murmiliuk, Peter **Košovan**, Miroslav Janata, Karel Procházka, Filip Uhlík, and Miroslav Štěpánek. Local pH and effective pK of a polyelectrolyte chain: Two names for one quantity? *ACS Macro Letters*, 7(10):1243–1247, 2018.
- [4] Jonas Landsgesell, Lucie Nová, Oleg Rud, Filip Uhlík, David Sean, Pascal Hebbeker, Christian Holm, and Peter **Košovan**. Simulations of ionization equilibria in weak polyelectrolyte solutions and gels. *Soft Matter*, 15(6):1155–1185, 2019.
- [5] Jonas Landsgesell, Pascal Hebbeker, Oleg Rud, Raju Lunkad, Peter **Košovan**, and Christian Holm. Grand-reaction method for simulations of ionization equilibria coupled to ion partitioning. *Macromolecules*, 53(8):3007–3020, 2020.
- [6] Raju Lunkad, Anastasiia Murmiliuk, Pascal Hebbeker, Milan Boublík, Zdeněk Tošner, Miroslav Štěpánek, and Peter **Košovan**. Quantitative prediction of charge regulation in oligopeptides. *Molecular Systems Design & Engineering*, 6(2):122–131, 2021.
- [7] Raju Lunkad, Anastasiia Murmiliuk, Zdeněk Tošner, Miroslav Štěpánek, and Peter **Košovan**. Role of pka in charge regulation and conformation of various peptide sequences. *Polymers*, 13(2):214, Jan 2021.
- [8] Roman Staňo, Peter **Košovan**, Andrea Tagliabue, and Christian Holm. Electrostatically cross-linked reversible gels – effects of pH and ionic strength. *Macromolecules*, 2021.

References to other works

- [9] Mikael Lund and Bo Jönsson. Charge regulation in biomolecular solution. *Quarterly reviews of biophysics*, 46(3):265–8, 08 2013.
- [10] A. Katchalsky and J. Gillis. Theory of the potentiometric titration of polymeric acids. *Rec. Trav. Chim.*, 68(6):879, 1949.
- [11] R. Israëls, F. A. M. Leermakers, and G. J. Fleer. On the theory of grafted weak polyacids. *Macromolecules*, 27(11):3087–3093, 1994.
- [12] G. S. Hartley and J. W. Roe. Ionic concentrations at interfaces. *Trans. Faraday Soc.*, 35:101–109, 1940.
- [13] R. Arnold. The titration of polymeric acids. *Journal of Colloid Science*, 12(6):549–556, 1957.
- [14] Barry W. Ninham and V. Adrian Parsegian. Electrostatic potential between surfaces bearing ionizable groups in ionic equilibrium with physiologic saline solution. *Journal of Theoretical Biology*, 31(3):405–428, June 1971.
- [15] Martin Müller, Luise Wirth, and Birgit Urban. Determination of the Carboxyl Dissociation Degree and pK_a Value of Mono and Polyacid Solutions by FTIR Titration. *Macromolecular Chemistry and Physics*, 222(4):2000334, February 2021.
- [16] Mathias A.S. Hass and Frans A.A. Mulder. Contemporary NMR Studies of Protein Electrostatics. *Annual Review of Biophysics*, 44(1):53–75, June 2015. tex.ids: hass2015a.
- [17] Fernando Luís Barroso da Silva and Donal MacKernan. Benchmarking a Fast Proton Titration Scheme in Implicit Solvent for Biomolecular Simulations. *Journal of Chemical Theory and Computation*, 13(6):2915–2929, 2017.
- [18] Motoyoshi Ikebuchi, Atsunori Kashiwagi, Takayuki Asahina, Yasushi Tanaka, Yoshihumi Takagi, Yoshihiko Nishio, Hideki Hidaka, Ryuichi Kikkawa, and Yukio Shigeta. Effect of medium ph on glutathione redox cycle in cultured human umbilical vein endothelial cells. *Metabolism*, 42(9):1121 – 1126, 1993.
- [19] William Nicholas Ainis, Adeline Boire, Véronique Solé-Jamault, Aurélie Nicolas, Said Bouhallab, and Richard Ipsen. Contrasting assemblies of oppositely charged proteins. *Langmuir*, 35(30):9923–9933, Jul 2019.
- [20] K Ulbrich. Polymeric anticancer drugs with ph-controlled activation. *Advanced Drug Delivery Reviews*, 56(7):1023–1050, Apr 2004.
- [21] Jéré J. van Lente, Mireille M. A. E. Claessens, and Saskia Lindhoud. Charge-based separation of proteins using polyelectrolyte complexes as models for membraneless organelles. *Biomacromolecules*, 20(10):3696–3703, Aug 2019.
- [22] Uwe Freudenberg, Passant Atallah, Yanuar Dwi Putra Limasale, and Carsten Werner. Charge-tuning of glycosaminoglycan-based hydrogels to program cytokine sequestration. *Faraday Discussions*, 219:244–251, 2019.
- [23] Lucas Schirmer, Karolina Chwalek, Mikhail V. Tsurkan, Uwe Freudenberg, and Carsten Werner. Glycosaminoglycan-based hydrogels with programmable host reactions. *Biomaterials*, 228:119557, Jan 2020.

- [24] Somdeb Jana and Mariusz Uchman. Poly(2-oxazoline)-based Stimulus-Responsive (Co)polymers: An Overview of their Design, Solution Properties, Surface-chemistries and Applications. *Progress in Polymer Science*, page 101252, 2020.
- [25] Florian Weik, Rudolf Weeber, Kai Szuttor, Konrad Breitsprecher, Joost de Graaf, Michael Kuron, Jonas Landsgesell, Henri Menke, David Sean, and Christian Holm. ESPResSo 4.0 – an extensible software package for simulating soft matter systems. *The European Physical Journal Special Topics*, 227(14):1789–1816, 2019.
- [26] Daniel T Gillespie. A general method for numerically simulating the stochastic time evolution of coupled chemical reactions. *Journal of computational physics*, 22(4):403–434, 1976.
- [27] Daniel T Gillespie. Stochastic simulation of chemical kinetics. *Annu. Rev. Phys. Chem.*, 58:35–55, 2007.
- [28] William R. Smith and Weikai Qi. Molecular simulation of chemical reaction equilibrium by computationally efficient free energy minimization. *ACS Central Science*, 4(9):1185–1193, Aug 2018.
- [29] Josep L. Garcés, Sergio Madurga, Carlos Rey-Castro, and Francesc Mas. Dealing with long-range interactions in the determination of polyelectrolyte ionization properties. extension of the transfer matrix formalism to the full range of ionic strengths. *Journal of Polymer Science Part B: Polymer Physics*, 55(3):275–284, Nov 2016.
- [30] Pablo M. Blanco, Sergio Madurga, Francesc Mas, and Josep L. Garcés. Coupling of Charge Regulation and Conformational Equilibria in Linear Weak Polyelectrolytes: Treatment of Long-Range Interactions via Effective Short-Ranged and pH-Dependent Interaction Parameters. *Polymers*, 10(8):811, August 2018. Number: 8 Publisher: Multidisciplinary Digital Publishing Institute.
- [31] John Mongan, David A. Case, and J. Andrew McCammon. Constant pH molecular dynamics in generalized born implicit solvent. *Journal of Computational Chemistry*, 25(16):2038–2048, dec 2004.
- [32] Adri CT Van Duin, Siddharth Dasgupta, Francois Lorant, and William A Goddard. Reaxff: a reactive force field for hydrocarbons. *The Journal of Physical Chemistry A*, 105(41):9396–9409, 2001.
- [33] Ana Damjanovic, Benjamin T Miller, Asim Okur, and Bernard R Brooks. Reservoir ph replica exchange. *The Journal of Chemical Physics*, 149(7):072321, 2018.
- [34] Jonas Landsgesell, Christian Holm, and Jens Smiatek. Wang–landau reaction ensemble method: Simulation of weak polyelectrolytes and general acid–base reactions. *Journal of Chemical Theory and Computation*, 13(2):852–862, 2017.
- [35] Martin Lísal, John K Brennan, William R Smith, and Flor R Siperstein. Dual control cell reaction ensemble molecular dynamics: a method for simulations of reactions and adsorption in porous materials. *The Journal of chemical physics*, 121(10):4901–4912, 2004.
- [36] C Heath Turner, John K Brennan, Martin Lísal, William R Smith, J Karl Johnson, and Keith E Gubbins. Simulation of chemical reaction equilibria by the reaction ensemble monte carlo method: a review. *Molecular Simulation*, 34(2):119–146, 2008.

- [37] Inderdip Shere and Ateeque Malani. Polymerization kinetics of a multi-functional silica precursor studied using a novel monte carlo simulation technique. *Physical Chemistry Chemical Physics*, 20(5):3554–3570, 2018.
- [38] Wei Chen, Brian H. Morrow, Chuanyin Shi, and Jana K. Shen. Recent development and application of constant ph molecular dynamics. *Molecular Simulation*, 40(10-11):830–838, May 2014.
- [39] John Mongan and David A Case. Biomolecular simulations at constant ph. *Current opinion in structural biology*, 15(2):157–163, 2005.
- [40] Daan Frenkel and Berend Smit. *Understanding Molecular Simulation*. Academic Press, San Diego, second edition, 2002.
- [41] Christopher E. Reed and Wayne F. Reed. Monte carlo study of titration of linear polyelectrolytes. *The Journal of Chemical Physics*, 96(2):1609–1620, 1992.
- [42] Jonas Landsgesell, Christian Holm, and Jens Smiatek. Simulation of weak polyelectrolytes: a comparison between the constant ph and the reaction ensemble method. *The European Physical Journal Special Topics*, 226(4):725–736, 2017.
- [43] A.Z. Panagiotopoulos. Charge correlation effects on ionization of weak polyelectrolytes. *Journal of Physics: Condensed Matter*, 21:424113, 2009.
- [44] S. Uyaver and C. Seidel. Effect of varying salt concentration on the behaviour of weak polyelectrolytes in a poor solvent. *Macromolecules*, 42:1352–1361, 2009.
- [45] S. Uyaver and C. Seidel. First-order conformational transtition of annealed polyelectrolytes in a poor solvent. *Europhysics Letters*, 64(4):536–542, 2003.
- [46] S. Uyaver and C. Seidel. Pearl-necklace structures in annealed polyelectrolytes. *J. Phys. Chem. B.*, 108:18804–18814, 2004.
- [47] Fabrice Carnal, Serge Ulrich, and Serge Stoll. Influence of explicit ions on titration curves and conformations of flexible polyelectrolytes: A Monte Carlo study. *Macromolecules*, 43(5):2544–2553, 2010.
- [48] Fabrice Carnal and Serge Stoll. Adsorption of weak polyelectrolytes on charged nanoparticles. impact of salt valency, ph, and nanoparticle charge density. monte carlo simulations. *The Journal of Physical Chemistry B*, 115(42):12007—12018, Oct 2011.
- [49] Arnaud Clavier, Marianne Seijo, Fabrice Carnal, and Serge Stoll. Surface charging behavior of nanoparticles by considering site distribution and density, dielectric constant and ph changes – a monte carlo approach. *Physical Chemistry Chemical Physics*, 17(6):4346–4353, 2015.
- [50] Arnaud Clavier, Fabrice Carnal, and Serge Stoll. Effect of surface and salt properties on the ion distribution around spherical nanoparticles: Monte carlo simulations. *The Journal of Physical Chemistry B*, 120(32):7988–7997, Aug 2016.
- [51] W. R. Smith and B. Třiska. The reaction ensemble method for the computer simulation of chemical and phase equilibria. I. Theory and basic examples. *Journal of Chemical Physics*, 100(4):3019–3027, 1994.
- [52] J Karl Johnson, Athanassios Z Panagiotopoulos, and Keith E Gubbins. Reactive canonical monte carlo: a new simulation technique for reacting or associating fluids. *Molecular Physics*, 81(3):717–733, 1994.

- [53] John P. Valleau and L. Kenneth Cohen. Primitive model electrolytes. i. grand canonical monte carlo computations. *The Journal of Chemical Physics*, 72(11):5935–5941, Jun 1980.
- [54] Filip Uhlík, Peter Košovan, Zuzana Limpouchová, Karel Procházka, Oleg V. Borisov, and Frans A. M. Leermakers. Modeling of ionization and conformations of starlike weak polyelectrolytes. *Macromolecules*, 47(12):4004–4016, 2014.
- [55] J. Klein Wolterink, J. van Male, M. A. Cohen Stuart, L. K. Koopal, E. B. Zhulina, and O. V. Borisov. Annealed star-branched polyelectrolytes in solution. *Macromolecules*, 35:9176–9190, 2002.
- [56] MB Ewing, TH Lilley, GM Olofsson, MT Ratzsch, and G Somsen. Standard quantities in chemical thermodynamics. fugacities, activities and equilibrium constants for ζ —pure and mixed phases (iupac recommendations 1994). *Pure and Applied Chemistry*, 66(3):533–552, 1994.
- [57] R. Israëls, F. A. M. Leermakers, G. J. Fleer, and E. B. Zhulina. Charged polymeric brushes: Structure and scaling relations. *Macromolecules*, 27(12):3249–3261, 1994.
- [58] Tomer Markovich, David Andelman, and Rudi Podgornik. Charged membranes: Poisson-boltzmann theory, dlvo paradigm and beyond. *arXiv preprint arXiv:1603.09451*, 2016.
- [59] E. B. Zhulina and O. V. Borisov. Poisson–boltzmann theory of ph-sensitive (annealing) polyelectrolyte brush. *Langmuir*, 27(17):10615–10633, 2011.
- [60] P. Biehl, P. Wiemuth, J. Garcia Lopez, M.-C. Barth, A. Weidner, S. Dutz, K. Peneva, and F. H. Schacher. Weak Polyampholytes at the Interface of Magnetic Nanocarriers: A Facile Catch-and-Release Platform for Dyes. *Langmuir*, 36(22):6095–6105, 2020.
- [61] Mariusz Uchman, Miroslav Štěpánek, Karel Procházka, Grigoris Mountrichas, Stergios Pispas, Ilja K. Voets, and Andreas Walther. Multicompartment Nanoparticles Formed by a Heparin-Mimicking Block Terpolymer in Aqueous Solutions. *Macromolecules*, 42(15):5605–5613, 2009.
- [62] Roman Staňo Roman. Effect of acid-base equilibria on the association behaviour of polyelectrolytes. Master’s thesis, Charles University, Prague, 2020.
- [63] F. G. Donnan. The theory of membrane equilibria. *Chemical Reviews*, 1(1):73–90, 1924.
- [64] J. Rička and Toyochi Tanaka. Swelling of ionic gels: quantitative performance of the donnan theory. *Macromolecules*, 17(12):2916–2921, 1984.
- [65] A Philipse and A Vrij. The donnan equilibrium: I. on the thermodynamic foundation of the donnan equation of state. *Journal of Physics: Condensed Matter*, 23(19):194106, 2011.
- [66] R. P. Buck, S. Rondinini, A. K. Covington, F. G. K. Baucke, C. M. A. Brett, M. F. Camoes, M. J. T. Milton, R. Mussini, R. Naumann, K. W. Pratt, P. Spitzer, and G. S. Wilson. Measurement of ph. definition, standards, and procedures (iupac recommendations 2002). *Pure and Applied Chemistry*, 74(11):2169, 2002.

- [67] Roberto Fernandez-Alvarez, Vladimír Ďorđovič, Mariusz Uchman, and Pavel Matějček. Amphiphiles without head-and-tail design: Nanostructures based on the self-assembly of anionic boron cluster compounds. *Langmuir*, 34(12):3541–3554, 2018. PMID: 29144761.
- [68] Paul J. Flory and Jr. John Rehner. Statistical mechanics of cross-linked polymer networks ii. swelling. *The Journal of Chemical Physics*, 11(11):521–526, 1943.

